Molecular Cell

Article

Crystal Structure of the LSD1/CoREST Histone Demethylase Bound to Its Nucleosome Substrate

Graphical Abstract

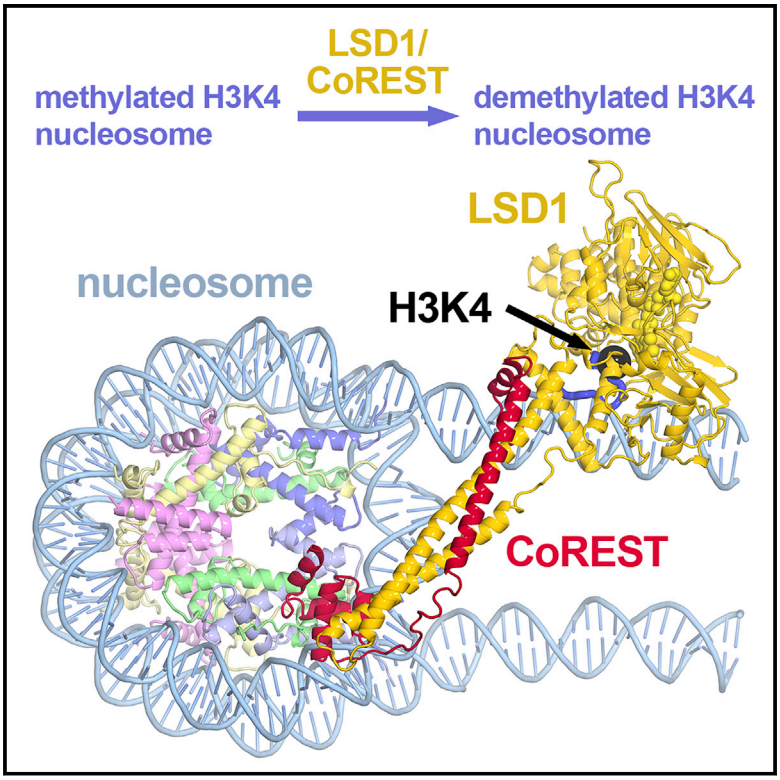

Highlights

- The structure explains why CoREST is necessary for LSD1 to demethylate nucleosomes
- LSD1 unexpectedly binds to extranucleosomal/linker DNA away from the nucleosome core
- The LSD1(K661A) putative catalytically inactive mutant is active on nucleosomes
- LSD1 can bind to two distinct sites on the nucleosome

Authors

Sang-Ah Kim, Jiang Zhu,
Neela Yennawar, Priit Eek, Song Tan

Correspondence

sxt30@psu.edu

In Brief

This crystal structure shows how the LSD1/CoREST histone demethylase binds to its nucleosome substrate to remove the transcriptionally active histone H3 Lys4 methyl mark. This study describes the mechanistic basis for how a non-catalytic accessory subunit (CoREST) enables a catalytic subunit (LSD1) to function on a nucleosome substrate.

Kim et al., 2020, Molecular Cell *78*, 1–12
June 4, 2020
https://doi.org/10.1016/j.molcel.2020.04.019

CellPress

Molecular Cell

CellPress

Article

Crystal Structure of the LSD1/CoREST Histone Demethylase Bound to Its Nucleosome Substrate

Sang-Ah Kim,[1,3] Jiang Zhu,[1,3] Neela Yennawar,[2] Priit Eek,[1] and Song Tan[1,4,*]

[1]Department of Biochemistry and Molecular Biology, Center for Eukaryotic Gene Regulation, The Pennsylvania State University, University Park, PA 16802, USA

[2]Huck Institutes of the Life Sciences, The Pennsylvania State University, University Park, PA 16802, USA

[3]These authors contributed equally

[4]Lead Contact

*Correspondence: sxt30@psu.edu

https://doi.org/10.1016/j.molcel.2020.04.019

SUMMARY

LSD1 (lysine specific demethylase; also known as KDM1A), the first histone demethylase discovered, regulates cell-fate determination and is overexpressed in multiple cancers. LSD1 demethylates histone H3 Lys4, an epigenetic mark for active genes, but requires the CoREST repressor to act on nucleosome substrates. To understand how an accessory subunit (CoREST) enables a chromatin enzyme (LSD1) to function on a nucleosome and not just histones, we have determined the crystal structure of the LSD1/CoREST complex bound to a 191-bp nucleosome. We find that the LSD1 catalytic domain binds extranucleosomal DNA and is unexpectedly positioned 100 Å away from the nucleosome core. CoREST makes critical contacts with both histone and DNA components of the nucleosome, explaining its essential function in demethylating nucleosome substrates. Our studies also show that the LSD1(K661A) frequently used as a catalytically inactive mutant *in vivo* (based on *in vitro* peptide studies) actually retains substantial H3K4 demethylase activity on nucleosome substrates.

INTRODUCTION

LSD1 (Lysine-Specific Demethylase; also known as KDM1A) is a critical regulator of cell-fate determination. It is required for embryonic development in mice and controls stem cell identity as well as differentiation pathways of diverse cell types (Foster et al., 2010; Hino et al., 2016; Whyte et al., 2012). It was the first histone demethylase identified and acts on mono- and dimethylated histone H3K4 as well as H3K9 and H4K20 (Metzger et al., 2005; Shi et al., 2004; Wang et al., 2015). LSD1 is overexpressed in many cancer cells and is, consequently, the active target of therapeutic interventions (Magliulo et al., 2018; Maiques-Diaz and Somervaille, 2016).

LSD1 acts as a transcriptional repressor when it erases the H3K4 methyl mark associated with transcriptional activation (Shi et al., 2004). LSD1's H3K4 histone demethylase activity maps to its flavin-dependent amine oxidase domain, and LSD1 is able to demethylate histone peptide substrates on its own (Forneris et al., 2005). However, LSD1 alone is not able to demethylate its physiological substrate, the nucleosome complex of histones and DNA. Like many histone modification enzymes, LSD1 interacts with other chromatin proteins that can regulate its enzymatic activity. LSD1 forms a stable complex with the CoREST co-repressor protein, and the LSD1/CoREST complex has robust H3K4 demethylase activity on nucleosome substrates (Lee et al., 2005; Shi et al., 2005).

Biochemical studies have defined the regions of LSD1 and CoREST required for demethylating histone H3K4 in nucleosomes, and structural studies have helped us visualize how these domains are organized (Chen et al., 2006; Stavropoulos et al., 2006; Yang et al., 2006). LSD1's catalytic amine oxidase domain is interrupted by a protruding α-helical tower domain that mediates coiled-coil interactions with CoREST. This interaction positions CoREST's SANT2 domain required for nucleosomal interactions away from the LSD1 catalytic domain. Crystal structures of LSD1/CoREST with H3 peptides show that the LSD1 catalytic pocket engages the first 16 residues of histone H3 and directs mono- or di-methylated H3K4 toward the flavin FAD for catalysis (Amano et al., 2017; Forneris et al., 2007; Yang et al., 2007). However, while these studies have provided valuable insight into how LSD1 catalyzes an H3K4 peptide substrate, they do not explain how LSD1 and CoREST work together to demethylate H3K4 in the physiologically pertinent nucleosome substrate.

We have crystallized LSD1/CoREST in complex with the nucleosome containing linker or extranucleosomal DNA. Our structure shows that the LSD1 catalytic domain binds not to the nucleosome itself but to extranucleosomal DNA away from the nucleosome core. Interactions with the nucleosome core

Please cite this article in press as: Kim et al., Crystal Structure of the LSD1/CoREST Histone Demethylase Bound to Its Nucleosome Substrate, Molecular Cell (2020), https://doi.org/10.1016/j.molcel.2020.04.019

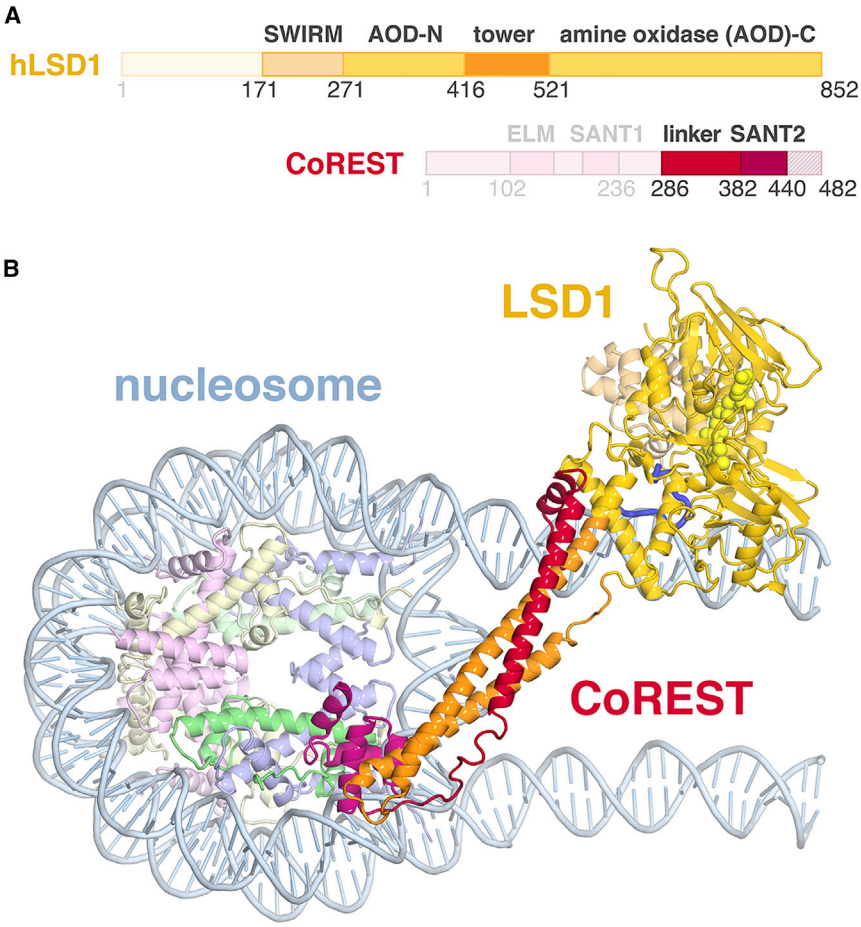

Figure 1. Structure of LSD1/CoREST/Nucleosome Complex

(A) Cartoon representation of human LSD1 and CoREST primary structure. Regions not present in the LSD1/CoREST protein complex used are shown faded out.

(B) Ribbon representation of LSD1/CoREST/nucleosome crystal structure at 5-Å resolution. LSD1 and CoREST domains are colored as in (A). Histones H2A, H2B, H3, and H4 and nucleosomal DNA are indicated in light yellow, pink, cornflower blue, light green, and light blue, respectively. The histone H3 tail in the LSD1 catalytic pocket is highlighted as a thicker tube in blue. Only one representative LSD1/CoREST molecule on a nucleosome is indicated for clarity.

are mediated by CoREST, providing the mechanistic basis for how CoREST enables LSD1 to function on the nucleosome. We also observe a second binding site for LSD1, but not for CoREST, on the nucleosome both in the crystal and in solution.

RESULTS

Crystallization and Structure Determination of LSD1/CoREST/Nucleosome Complexes

Since our enzymatic studies showed that LSD1/CoREST was significantly more active on nucleosome substrates containing extranucleosomal DNA, and since we found that LSD1/CoREST bound nucleosomes more tightly with 5 to 31 bp of extranucleosomal DNA on either side of the nucleosome (Kim et al., 2015), we conducted crystallization trials of LSD1/CoREST bound to 155- to 207-bp nucleosomes. We used the same human LSD1(171–852) and CoREST(286–482) truncations used previously for structural and biochemical studies (Yang et al., 2006) (Figure 1A), and we also explored using the CoREST(286–440) that removes the unstructured CoREST C terminus. For nucleosomes, we used 15 nucleosomes containing symmetrically positioned extranucleosomal DNA (using the Widom 601 nucleosome positioning sequence) and 6 nucleosomes with extranucleosomal DNA only on one side. Of the resulting 81 different LSD1/CoREST/nucleosome variants, 34 produced crystals. Nine variants produced crystals that diffracted X-rays to better than 7 Å. The best diffraction to 5.0 Å was obtained from a LSD1(171–852)/CoREST(286–440)/191-bp nucleosome complex. The LSD1 in this complex also contained the engineered R608A, N717A, and D721A mutations (m5 mutation in Figure 2) that we thought might improve crystal packing and that did not affect catalytic activity. The nucleosome in this complex contained the 145-bp Widom 601 nucleosome core positioning sequence flanked by 23 bp of extranucleosomal DNA on either side. We also used the H3 K4M mutation that increases the binding affinity of LSD1/CoREST to nucleosomes by 30-fold (Forneris et al., 2007).

We solved the structure of the LSD1/CoREST/nucleosome using the LSD1/CoREST complex and the nucleosome core particle as molecular replacement search models (Table 1). The asymmetric unit contains two nucleosomes each with two molecules of LSD1/CoREST bound (Figure S1A). At 5.0 Å resolution, the orientation of LSD1/CoREST on the nucleosome is clear, as are the secondary structure elements (Figure S2A). Although electron densities for amino-acid side chains are very weak at best, the availability of high-resolution structures of the LSD1/CoREST complex and the nucleosome allowed us to build and refine an atomic model for the LSD1/CoREST/nucleosome complex. While we might not be able to visualize amino-acid side chains in the electron density map, the atomic model allows us to propose likely interactions between the LSD1/CoREST enzyme and its nucleosome substrate. We believe that the long extranucleosomal DNA in the LSD1/CoREST/nucleosome complex makes it difficult to tightly pack the complex in a crystal and consequently limits the diffraction resolution of the crystals.

Overview of LSD1/CoREST/Nucleosome Structure

Our crystal structure shows that LSD1/CoREST binds to each of the histone, DNA, and extranucleosomal DNA components of

Please cite this article in press as: Kim et al., Crystal Structure of the LSD1/CoREST Histone Demethylase Bound to Its Nucleosome Substrate, Molecular Cell (2020), https://doi.org/10.1016/j.molcel.2020.04.019

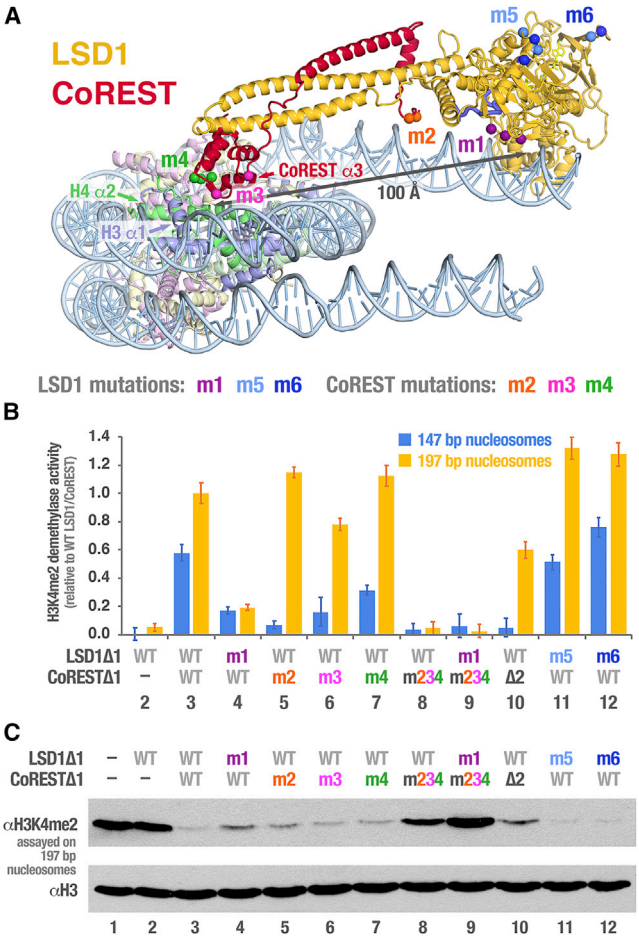

Figure 2. Mutational Analysis of LSD1/CoREST Validates Interactions with the Nucleosome

(A) Locations of residues interrogated by mutational analysis. The Cα positions of LSD1 m1 (K355A, K357A, and K359A), LSD1 m5 (R608A, N717A, and D721A), LSD1 m6 (S609E, S719E, and G725E), CoREST m2 (K309E and K312E), CoREST m3 (K378E and R382E), and CoREST m4 (R425E, R426E, and R427E) mutations are indicated in purple, light blue, blue, orange, pink, and green respectively.

(B) Histone demethylase activity of LSD1Δ1/CoRESTΔ1 variants analyzed by peroxidase-linked assay using 147- and 197-bp H3K$_c$4 nucleosome substrates. CoRESTΔ2, CoREST(316–440), i.e., lacking residues 286–315. Plotted values (mean ± SEM) have been corrected for background counts in the absence of added LSD1/CoREST enzyme.

(C) Histone demethylase activity analyzed by western blotting using anti-H3K4me2 antibodies and reprobed using anti-H3 antibodies. A weak anti-H3K4me2 signal corresponds to strong demethylase activity.

the nucleosome (Figure 1B). The LSD1 amine-oxidase domain interacts with the phosphate backbone of extranucleosomal DNA 1.5 to 2 turns from the nucleosome core. The catalytic domain also binds the H3 tail, as previously observed in LSD1 structures with H3 peptides (Amano et al., 2017; Forneris et al., 2007; Yang et al., 2007). The CoREST subunit interacts with two distinct regions of the nucleosome as well. The N-terminal region of the CoREST linker that precedes the SANT2 domain binds the extranucleosomal DNA about 1 turn from the nucleosome core, while the SANT2 domain binds to histone H4 on the octamer face of the nucleosome as well as to nucleosomal DNA about 1.5 turns from the nucleosomal dyad. The LSD1 tower domain intertwined with the CoREST linker region forms a bridge between the LSD1 and CoREST interactions with extranucleosomal DNA and the CoREST SANT2 domain interactions with the histone octamer surface. These individual interactions position the LSD1 catalytic domain on extranucleosomal DNA away from the nucleosome core and on the nucleosome side distal to where the CoREST SANT2 domain binds.

Two key aspects of the crystal structure of LSD1/CoREST bound to the nucleosome differ from previously published models for the enzyme/nucleosome complex: the LSD1 catalytic domain binds directly to extranucleosomal DNA, and the CoREST SANT2 domain interacts with both the histone octamer surface and with nucleosomal DNA. Previous structural models for the LSD1/CoREST/nucleosome complex postulated that the CoREST SANT2 domain would bind to the major groove of DNA in analogy to the related myb DNA-binding domain. Yang et al. (2006) proposed that the CoREST SANT2 domain would bind to nucleosomal DNA 4.5 turns from the nucleosome dyad, positioning the LSD1 amine oxidase domain close to the H3 tail as it emerges from the nucleosome core (Figure S3A). Pilotto et al. (2015) combined small-angle X-ray scattering and mutagenesis studies to suggest that the CoREST SANT2 domain first binds DNA close to the nucleosome dyad, allowing the LSD1 amine oxidase domain to then capture the H3 tail without the need for the LSD1 amine oxidase domain to directly contact other regions of the nucleosome (Figure S3B).

The Yang and Pilotto structural models assumed that LSD1/CoREST binds to the nucleosome as a rigid body, but we observe that the CoREST SANT2 and the LSD1 amine oxidase domains each rotate approximately 5° inward to tighten the vise-clamp-like LSD1/CoREST structure when it binds in the nucleosome (Figures S3C–S3H). These distortions enable LSD1's amine oxidase domain to bind the extranucleosomal DNA while the CoREST SANT2 domain simultaneously engages the nucleosome core. In the absence of this conformational change, the LSD1 amine oxidase domain would be displaced about 5 Å away from the extranucleosomal DNA while the CoREST SANT2 domain would be displaced about 4 Å away from the nucleosome core, precluding the respective interactions. Similar motions of the LSD1 amine oxidase and CoREST SANT2 were observed in molecular dynamic simulation studies of LSD1/CoREST (Baron and Vellore, 2012). The omit electron density maps excluding the CoREST SANT2 domain provide assurance that the CoREST SANT2 domain has been properly positioned in the crystal structure (Figure S2B).

Our structure does not provide a role for the LSD1 SWIRM domain in nucleosome recognition: the SWIRM domain is positioned away from the nucleosome core and extranucleosomal DNA (Figure 1B).

LSD1 and CoREST Interactions with Extranucleosomal DNA

We have previously shown that extranucleosomal DNA significantly enhances the nucleosomal H3K4 demethylase activity

Please cite this article in press as: Kim et al., Crystal Structure of the LSD1/CoREST Histone Demethylase Bound to Its Nucleosome Substrate, Molecular Cell (2020), https://doi.org/10.1016/j.molcel.2020.04.019

of LSD1/CoREST (Kim et al., 2015). The crystal structure suggests a mechanistic explanation for this observation: LSD1 amine oxidase Lys355, Lys357, and Lys359 (Figure 2A, m1 sites) and Arg568 side chains are positioned to interact with the extranucleosomal DNA 15 to 20 bp beyond the nucleosome core. Furthermore, the N-terminal region of the CoREST linker presents Lys309 and Lys312 (Figure 2A, m2 sites) close to the DNA backbone 10 to 12 bp beyond the nucleosome core. These interactions on the extranucleosomal DNA are consistent with photocrosslinking studies between LSD1/CoREST and nucleosomes containing extranucleosomal DNA (Kim et al., 2015).

CoREST Interactions with the Nucleosome Core

LSD1's and CoREST's interactions with extranucleosomal DNA are complemented by CoREST SANT2 domain interactions with the nucleosome core 100 Å away (Figure 2A). The C-terminal region of the CoREST SANT2 domain α3 helix and the short 3_{10} helix that follows interact with histone H4 residues 26–29 preceding the histone fold, while Arg426 from the SANT2 3_{10} helix is in position to interact with both the H4 histone fold α2 helix and the histone H3 α1 helix. In addition to these protein-protein interactions are SANT2 domain interactions near where the H3 L1-H4 L2 histone fold binds to nucleosomal DNA two turns from the nucleosome dyad. These DNA interactions appear to be mediated by CoREST residues Lys378 and Arg382 (Figure 2A, m3 sites) at the boundary or just preceding the SANT2 domain and Gln416 in the SANT2 domain α3 helix. The SANT domain-DNA interactions are significantly different from how the structurally related myb DNA-binding domain binds to DNA (Yang et al., 2006) (Figures S4A–S4F). While myb DNA-binding domains insert their α3 helix into the DNA major groove, the SANT2 domain does not, precluding CoREST SANT2 residues Trp383 and Asn419 from binding to DNA (the analogous residues in myb bind to DNA).

Biochemical Validation of LSD1/CoREST Interactions with the Nucleosome

Given the difficulty in visualizing amino-acid side chains at the limited resolution of our crystal structure, it was particularly important to validate the contacts mediating the interactions between LSD1/CoREST and the nucleosome. We useded two assays for LSD1's histone demethylase activity: a peroxidase-coupled assay that measures hydrogen peroxide produced during LSD1-dependent lysine demethylation (Kim et al., 2015) (Figure 2B) and western blotting using anti-H3me2 antibodies (Figure 2C). Both assays used recombinant nucleosome substrates containing a methyl lysine analog of dimethylated H3 Lys4 ($H3K_c4me2$). Our results confirm that LSD1 requires CoREST to demethylate nucleosome substrates and that LSD1/CoREST has higher activity on nucleosomes containing extranucleosomal DNA (197 bp versus 147 bp) (Figure 2B, lane 3). Mutating LSD1 Lys355, Lys357, and Lys359, which form a basic stripe along the amine oxidase domain (mutation m1), reduces LSD1/CoREST activity approximately 3-fold on nucleosomes without significant extranucleosomal DNA and 5-fold on 197-bp nucleosomal DNA (26-bp extranucleosomal DNA on either side of the 145-bp Widom 601 nucleosome core) (Figure 2B, lane 4). This result confirms the importance of these three LSD1 residues in binding extranucleosomal DNA, since LSD1/CoREST's activity is reduced and the extranucleosomal DNA dependence is lost. The 3-fold reduction of activity of the m1 mutant on 147-bp nucleosome core particles in the absence of extranucleosomal DNA is consistent with a proposed role for Lys355, Lys357, and Lys359 to regulate H3 tail binding: molecular dynamics calculations suggest that these residues may affect H3 tail entry into LSD1's substrate binding pocket (Baron and Vellore, 2012).

The effects of mutating CoREST residues identified in our crystal structure are consistent with a critical role for CoREST in interacting with the nucleosome. Mutating CoREST residues Lys309 and Lys312 at the N terminus of the linker region (mutation m2) significantly reduces demethylase activity on 147-bp nucleosomes but not on 197-bp nucleosomes (Figure 2B, lane 5). This suggests that the LSD1 amine oxidase may be more important than the CoREST linker for binding nucleosomes with extranucleosomal DNA. However, the much stronger effect of mutating CoREST Lys309 and Lys312 on 147-bp nucleosomes (approximately 9-fold reduction relative to wild-type LSD1/CoREST on 147-bp nucleosomes) indicates that these CoREST residues play an important role in the absence of extranucleosomal DNA. Similarly, we find that mutating CoREST SANT domain residues Lys378 and Arg382 (mutation m3), also predicted to bind nucleosomal DNA in our structure, likewise decreased demethylase activity on 147-bp nucleosomes (Figure 2B, lane 6), consistent with a possible role for CoREST SANT2 DNA-binding residues in scanning nucleosomal DNA (Pilotto et al., 2015). Mutations of CoREST SANT domain residues identified as mediating histone contacts (m4 mutations: Arg425, Arg426, and Arg427) reduced demethylase activity approximately 2-fold on 147-bp nucleosomes without reducing activity on 197-bp nucleosomes (Figure 2B, lane 7). Combining the CoREST m2, m3, and m4 mutations with or without the LSD1 m1 mutation reduced LSD1/CoREST demethylase activity to less than 5% of wild-type activity (essentially undetectable) (Figure 2B, lanes 8 and 9).

The CoREST polypeptide used for our crystallography and biochemical studies contains about 20 residues (286–308) not modeled in LSD1/CoREST structures or in our LSD1/CoREST/nucleosome complex. To investigate whether these residues abundant with basic amino acids might be important for nucleosome demethylation, we prepared LSD1/CoRESTΔ2, which contains CoREST(316–440) but removes CoREST(286–308) as well as CoREST Lys309 and Lys312. We find that LSD1/CoRESTΔ2 further reduces H3K4 demethylation on both 147- and 197-bp nucleosome substrates (Figure 2B, lane 10), suggesting the possibility that residues within CoREST(286–308) may also interact with the nucleosome.

Analysis of LSD1 and CoREST mutations on demethylase activity by western blotting using anti-H3K4me2 antibodies (Figure 2C) largely confirms those using the peroxidase-coupled assay. Differences detected likely reflect distinctions between the peroxidase-coupled assay, which measures initial rates in the first 2 min, and the western blot assay, which measures product accumulation over 30 min.

Please cite this article in press as: Kim et al., Crystal Structure of the LSD1/CoREST Histone Demethylase Bound to Its Nucleosome Substrate, Molecular Cell (2020), https://doi.org/10.1016/j.molcel.2020.04.019

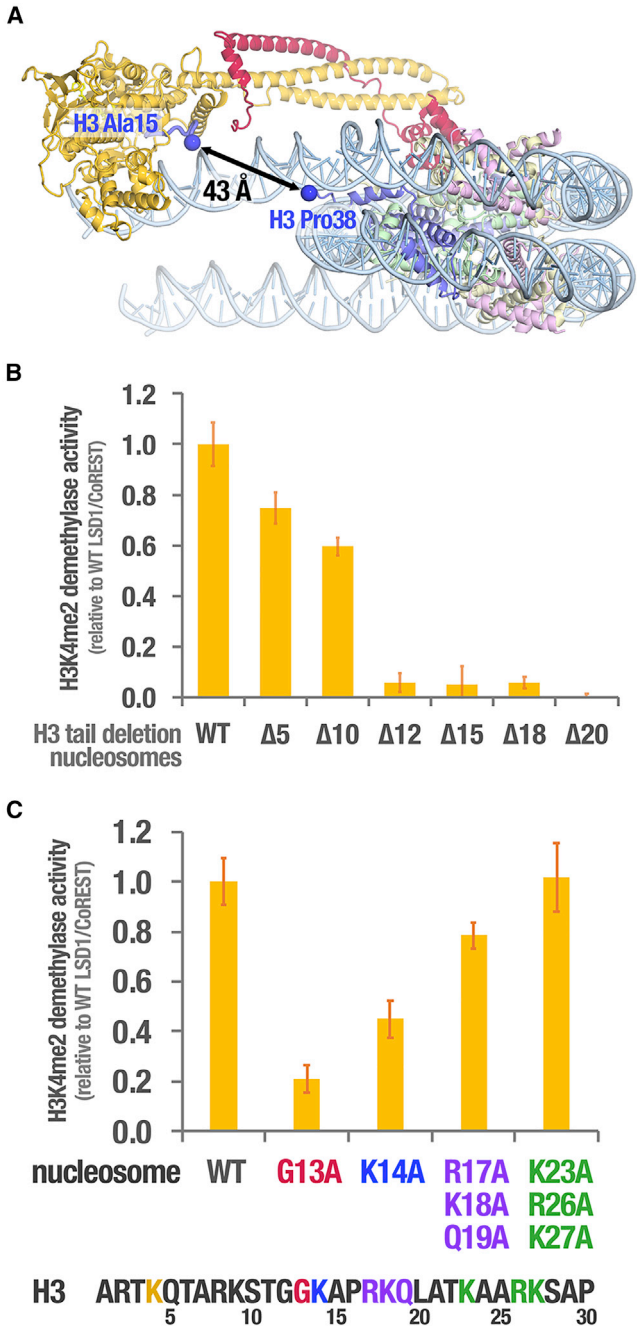

Figure 3. LSD1/CoREST Demethylase Activity on Nucleosomes Containing H3 Tail Truncations Are Consistent with the Crystal Structure

(A) LSD1/CoREST/nucleosome structure with histone H3 Ala15 and Pro38 Cα atoms indicated as blue spheres.

(B) Histone demethylase activity of LSD1Δ1/CoRESTΔ1 on 197-bp H3K_c4 nucleosome substrates containing deletions in the H3 tail starting at residue 21.

(C) Histone demethylase activity of LSD1Δ1/CoRESTΔ1 on 197-bp H3K_c4 nucleosome substrates containing histone H3 point mutations with sequence of the H3 tail (2–30) shown below. Data are presented as mean ± SEM.

Role of H3 Tail in LSD1/CoREST Nucleosome Demethylation Activity

The positioning of the LSD1 amine oxidase catalytic domain on extranucleosomal DNA 100 Å away from the nucleosome has implications for how LSD1 binds the H3 tail substrate to demethylate H3 Lys4. Crystal structures of LSD1/CoREST with N-terminal H3 peptides bound in the amine oxidase active site show that H3(1–15) are well structured. We observed electron density consistent with H3(1–15) in the LSD1 amine oxidase domain in our LSD1/CoREST/nucleosome structure (see the omit electron density map shown in Figures S2C and S2D), and next, we picked up density consistent with H3 for residue 38 as the H3 tail emerges from the nucleosome core particle. We did not observe electron density for the intervening H3 residues, but the observed distance of 43 Å between the C_α atoms of H3 Ala15 and Pro38 (Figure 3A) is less than the 84 Å that 24 amino acids from Ala15 to Pro38 could cover if in an extended conformation, assuming 3.5 Å per residue. This indicates that the H3 N-terminal tail has sufficient length to span the distance between emerging from the nucleosome core around superhelical location ±1 and entering the LSD1 amine oxidase domain (the H3 tail bound in the amine oxidase cannot originate from a neighboring nucleosome in the crystal, because all neighboring nucleosomes are too far away). Furthermore, the excess ~40 Å suggests that approximately 11 residues could be deleted from the H3 tail without necessarily impairing demethylase activity.

We tested this hypothesis by engineering deletions of different lengths into the H3 tail, starting with residue 21. We found that deletions of 5 of 10 residues are accommodated with reduction in demethylase activity of 25% and 40% on 197-bp nucleosomes, but further deletions of 12, 15, 18, and 20 residues reduce demethylase activity to less than 6% of 197-bp nucleosomes containing full-length H3 (Figure 3B). Similar results are observed using the western blot assay (Figures S5A and S5B). The dramatic reduction in demethylase for 10- versus 12-residue deletions is consistent with our crystal structure and provides evidence that the unexpected positioning of the LSD1 amine oxidase domain on extranucleosomal DNA away from the nucleosome core reflects the biologically active state.

The H3 deletions reduce the distance between the H3 N terminus and the H3 body, but the deletions also remove amino-acid side chains that could guide the H3 N-terminal peptide into the LSD1 active site, possibly by tracking along extranucleosomal DNA. For example, the 10-residue H3 tail deletion removes three basic residues: Lys23, Arg26, and Lys27 (Figure 3C). We found that removing the side chains of these three basic residues does not affect H3K_c4me2 demethylation activity on 197-bp nucleosomes (Figure 3C; Figure S5C), arguing against a role of these side chains in LSD1/CoREST demethylase activity. We also found that removing the side chains of H3 Arg17, Lys18, and Gln19 only slightly reduces LSD1/CoREST demethylase activity on 197-bp nucleosomes (Figure 3C; Figure S5C). While we are unable to model these residues in the crystal structure, the location of the H3 N-terminal tail residue 15 close to extranucleosomal DNA in our structure suggests the possibility that one or more of H3 Arg17, Lys18, and Gln19 may interact with extranucleosomal DNA.

Please cite this article in press as: Kim et al., Crystal Structure of the LSD1/CoREST Histone Demethylase Bound to Its Nucleosome Substrate, Molecular Cell (2020), https://doi.org/10.1016/j.molcel.2020.04.019

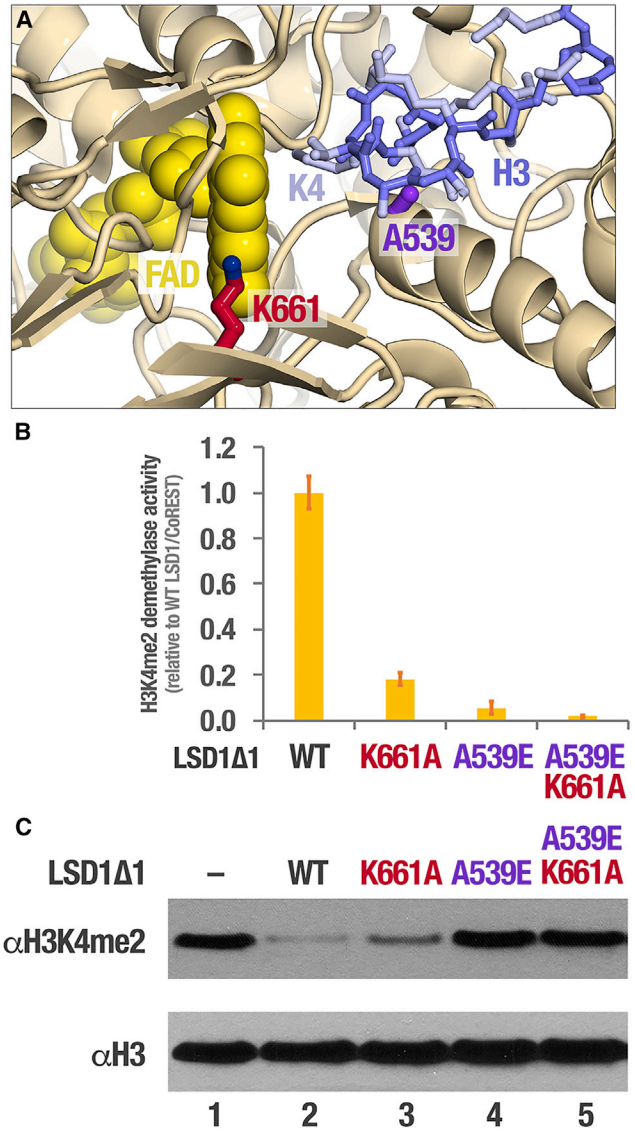

Figure 4. The LSD1(K661A)/CoREST Mutant Is Catalytically Active

(A) LSD1 K661 interacts with the FAD cofactor, while A539 interacts with the H3 peptide substrate, as observed in the 3.1-Å crystal structure of the LSD1Δ1/CoRESTΔ1/H3 peptide (Forneris et al., 2007).

(B) Histone demethylase activity (mean ± SEM) analyzed by peroxidase-linked assay of LSD1Δ1/CoRESTΔ1 complexes containing wild-type, K661A, A539A, or A539A+K661A LSD1 variants.

(C) Histone demethylase activity analyzed by anti-H3K4me2 western blotting. The significant reduction of $H3K_c4me2$ signal for the LSD1(K661A)/CoREST complex indicates that this complex is catalytically active. The assays in (B) and (C) used 197-bp $H3K_c4$ nucleosome substrates.

Acetylation of H3 Lys14 inhibits the $H3K_c4me2$ demethylase activity of the LSD1/HDAC1/CoREST demethylase-deacetylase complex (Wu et al., 2018). We find that the H3 Lys14Ala mutation reduces LSD1/CoREST $H3K_c4me2$ demethylase activity 2-fold in the peroxidase-linked assay (Figure 3C) and slightly in the western blot assay (Figure S5C). Our structure suggests a possible mechanistic role for the H3 Lys14 in LSD1 demethylase activity: in contrast to all other structures of H3 complexed to LSD1/CoREST, the H3 Lys14 side chain refines in a conformation to apparently interact with LSD1 Asp553 and Asp556 side chains and the Asp553 main chain (Figure S6). These interactions would be disrupted if H3 Lys14 were acetylated. We also found that adding a methyl group to H3 Gly13 causes an even stronger 5-fold reduction of LSD1/CoREST $H3K_c4me2$ demethylase activity (Figure 3C, G13A mutation). This deleterious effect can be explained by the close contact between H3 Gly13 and the LSD1(372–396) helix contact, which would be disrupted by the extra methyl group present in the Ala13 mutation.

The LSD1(K661A) Mutation Does Not Eliminate LSD1's $H3K_c4me2$ Demethylase Activity on Nucleosomes

The LSD1 Lys661 residue that interacts with the FAD cofactor (Figure 4A) has been identified as critical for LSD1's demethylase activity *in vitro* (Chen et al., 2006; Lee et al., 2005; Stavropoulos et al., 2006; Yang et al., 2006). Demethylase assays using peptide substrates show that the LSD1 K661A point mutant is abolished in H3K4 demethylase activity; consequently, the LSD1 K661A mutant has been widely used as a catalytically inactive LSD1 in *in vitro* and *in vivo* experiments. During studies to validate our nucleosome demethylase assays, we examined the LSD1(K661A)/CoREST point mutant, anticipating only background signal for this supposedly catalytically inactive mutant. We were, therefore, surprised to observe that LSD1(K661A)/CoREST retains approximately 20% of the demethylase initial rate activity of wild-type LSD1/CoREST in the peroxidase assay (Figure 4B). In contrast, the LSD1(A539E)/CoREST mutation that affects H3 tail substrate binding retains only about 5% of wild-type activity, and the LSD1(A539E/K661A)/CoREST double mutation's demethylase activity was not detectable (Figure 4B). The effects are even more dramatic in the western blot assay, which measures product accumulation: the K661A mutant was able to achieve demethylation almost similar to that of the wild-type enzyme, whereas little or no activity was detected for the A539E mutant (Figure 4C). We believe that the discrepancy of LSD1(K661A)/CoREST's demethylase activity arises from the use of peptide versus nucleosome substrates. The significant residual activity of the LSD1(K661A) mutant in H4K4me2 demethylation with the more physiological nucleosome substrates may account for puzzling results reported for the failure of the LSD1(K661A) to produce anticipated outcomes *in vivo* (Carnesecchi et al., 2017a; Hatzi et al., 2019; Maiques-Diaz et al., 2018b; Pilotto et al., 2016; Sehrawat et al., 2018). The LSD1(A539E/K661A) double mutation would be preferable as a catalytically impaired mutant in future studies.

A Second Binding Site for LSD1/CoREST on the Nucleosome

In addition to the LSD1/CoREST interaction with the nucleosome described earlier (hereinafter referred to as canonical binding), we observed a second binding mode in the crystal where a symmetry-related LSD1 interacts with the octamer face of the nucleosome (Figures 5A and 5B; Figures S1C and S1E). This crystal packing interaction enables two molecules of LSD1 to bind to one face of the nucleosome. CoREST does not interact with the nucleosome nor does LSD1 or CoREST interact with

Please cite this article in press as: Kim et al., Crystal Structure of the LSD1/CoREST Histone Demethylase Bound to Its Nucleosome Substrate, Molecular Cell (2020), https://doi.org/10.1016/j.molcel.2020.04.019

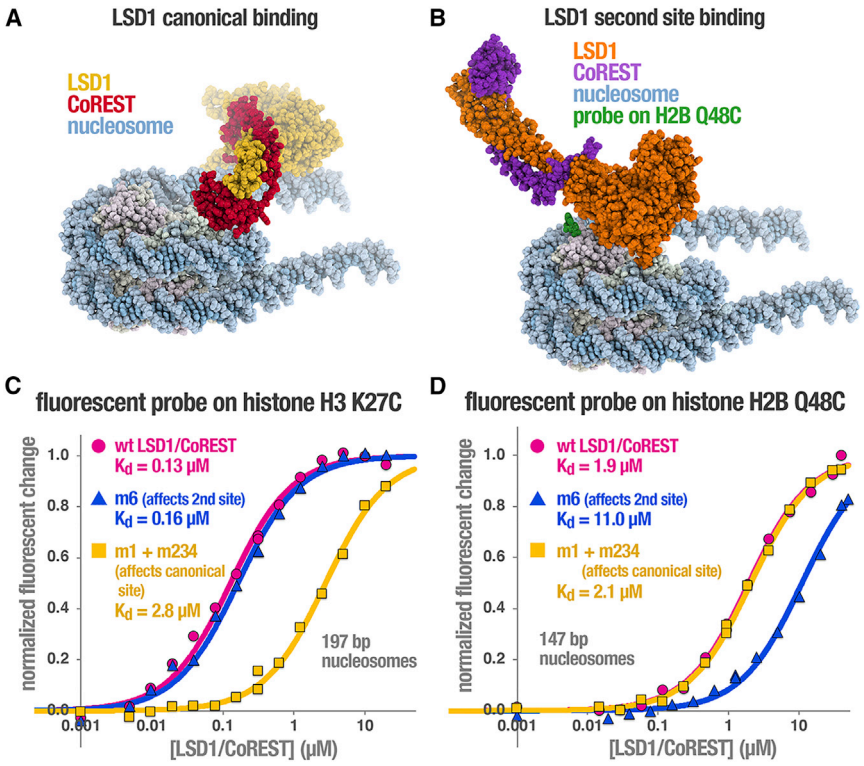

Figure 5. LSD1 Binds to the Nucleosome at Two Distinct Locations in the Crystal and in Solution

(A) "Canonical" binding of LSD1/CoREST to the nucleosome corresponds to the structure shown in Figures 1, 2, and 3.

(B) LSD1 interacts with a second site on the nucleosome in the crystal. The fluorescent probe (green) used to detect this second site binding is modeled at its H2B Q48C position.

(C) HI-FI nucleosome-binding assay shows that the combination of m1+m234 mutations that decreased H3K$_c$4me2 demethylase activity (Figure 2) has lower binding affinity to the nucleosome labeled on H3 K27C.

(D) HI-FI nucleosome fluorescently labeled on H2B Q48C shows a reversed effect: only the m6 mutation at the second LSD1/nucleosome site interface decreases binding affinity.

extranucleosomal DNA in this second binding mode. We initially dismissed this second binding site as a crystal packing artifact, but we subsequently found the same interaction in multiple LSD1/CoREST/nucleosome crystal forms in at least two different space groups and crystal packing arrangements (Figures S1B, S1D, and S1F).

To determine whether LSD1/CoREST can use these two different binding modes in solution, we examined the binding of LSD1/CoREST to nucleosomes with fluorescent probes engineered at specific histone positions using cysteine mutations. For the LSD1 canonical binding responsible for H3K4 demethylation, we used the same H3 K27C position used previously to characterize binding of LSD1/CoREST to the nucleosome. To detect the LSD1 second site binding, we labeled H2B Q48C close to the second site LSD1 catalytic domain (Figure 5B). We used the high-throughput interactions by fluorescence intensity (HI-FI) nucleosome-binding assay to monitor the quenching of the nucleosome fluorescent probe by the proximal binding of LSD1/CoREST. With the fluorescent probe on H3 K27C (canonical binding), we find that LSD1/CoREST binds to 197-bp nucleosomes with a dissociation constant (K_D) of 0.13 μM (Figure 5C, pink circles), very similar to our previous measurement of 0.135 μM for binding to 185-bp nucleosomes. With the fluorescent probe on H2B Q48C (second site binding), we detect binding of LSD1/CoREST to 147-bp nucleosomes with a dissociation constant of 1.9 μM (Figure 5D, pink circles) or 15-fold more weakly than the canonical binding, consistent with the more limited intermolecular interactions within the second binding site.

To confirm that the nucleosome binding detected using the H3 K27C and H2B Q48C probes correspond to the two binding modes detected in the crystal, we analyzed the same LSD1 and CoREST mutations used in the nucleosomal histone demethylase assays described earlier. We find that LSD1/CoREST bearing the LSD1 m1 and the CoREST m234 mutations is over 20-fold weaker in nucleosome binding compared to the wild-type LSD1/CoREST when assayed on H3 K27C-labeled nucleosomes (canonical binding) (Figure 5C, yellow squares). This result confirms the role of these mutated residues in canonical nucleosome binding. In contrast, LSD1/CoREST mutated on residues predicted to affect second-site binding (LSD1 m6 mutations) bound H3 K27C-labeled nucleosomes essentially identical to wild-type nucleosomes (for m6, K_D = 0.16 μM versus 0.13 μM for wild-type LSD1/CoREST) (Figure 5C, blue triangles). However, the effects of the mutations are reversed when assayed on H2B Q48C-labeled nucleosomes that detect second-site binding: the LSD1 m1 + CoREST m234 mutations now do not affect nucleosome binding (for m1 + m234, K_D = 2.1 μM versus 1.9 μM for wild-type LSD1/CoREST) (Figure 5D, yellow squares), but the LSD1 m6 mutations (S609E, S719E, and G725E) reduce nucleosome-binding affinity to 11.0 μM (Figure 5D, blue triangles). These results indicate that the two LSD1/CoREST binding modes to the nucleosome observed in the crystal also occur in solution. It should be noted that the LSD1 m6 mutations at the second binding site interface did not adversely affect H3K$_c$4me2 demethylation (Figures 2A and 2B, lane 12), providing evidence that LSD1 does not use the second binding site to demethylate H3K4me2. The slight increase in H3K$_c$4me2 demethylation activity of the LSD1(m6)/CoREST mutant might reflect reduced competition for nucleosome binding by reducing second-site binding.

LSD1 has been reported to demethylate H3K9me2 in an androgen-, estrogen-, or estrogen-related receptor (ERRα)-dependent manner (Carnesecchi et al., 2017b; Metzger et al., 2005; Nair et al., 2010). We therefore investigated whether LSD1 uses the second nucleosome binding site to demethylate

Please cite this article in press as: Kim et al., Crystal Structure of the LSD1/CoREST Histone Demethylase Bound to Its Nucleosome Substrate, Molecular Cell (2020), https://doi.org/10.1016/j.molcel.2020.04.019

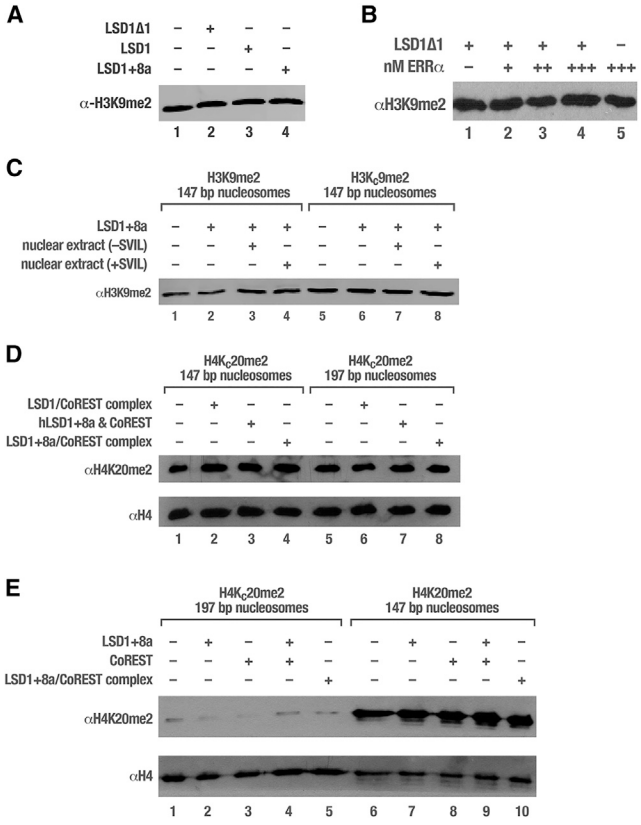

Figure 6. Western Blotting Data for Absence of H3K9me2 and H4K20me2 Histone Demethylation by LSD1 and LSD1+8a

(A) LSD1Δ1, LSD1, and LSD1+8a do not demethylate H3K$_c$9me2 nucleosomes.

(B) ERRα does not enable LSD1Δ1 to demethylate H3K$_c$9me2 nucleosomes. 200 nM H3Kc9me2 197-bp nucleosomes were incubated with 67 nM LSD1Δ1 and 0, 67, 133, or 200 nM recombinant ERRα.

(C) LSD1+8a does not demethylate H3K9me2 (Epicypher) or H3K$_c$9me2 nucleosomes with or without SVIL nuclear extracts.

(D) LSD1/CoREST, LSD1+8a + CoREST, and LSD1+8a/CoREST do not demethylate H4K$_c$20me2 147-bp or 197-bp nucleosomes.

(E) LSD1+8a and LSD1+8a/CoREST complex do not demethylate H4K$_c$20me2 197-bp or H4K20me2 147-bp (Epicypher) nucleosomes. The reduction in H4K$_c$20me2 signal in lane 2 is not reproducible and also occurs when the non-catalytic CoREST subunit is added (lane 3).

H3K9me2 in nucleosomes. We used the western blot assay to examine whether LSD1(172–852) or full-length LSD1 could demethylate H3K9me2 installed as methyl-lysine analog in nucleosomes (Figure 6A). Since ERRα was shown to enable LSD1 to demethylate H3K9me2, we also titrated ERRα in the demethylation reactions, but we still did not detect H3K$_c$9me2 demethylase activity, regardless of whether CoREST was present to stabilize LSD1 (Figure 6B; data not shown). Consequently, we were unable to determine whether LSD1's second nucleosomal binding site serves a biological function for LSD1 to demethylate H3K9me2.

A neuronal-specific isoform of LSD1—LSD1+8a, also known as LSD1n—is a splicing variant that adds 4 amino acids in the amine-oxidase catalytic domain (Laurent et al., 2015; Wang et al., 2015). This variant has been reported to regulate neuron development through H3K9me2 demethylation or to affect memory formation through H4K20 demethylation. The LSD1+8a variant has the same H3K4me2 demethylase activity as LSD1, and structural analysis of LSD1+8a shows that the additional 4 amino acids in LSD1+8a extends a loop region distant from the LSD1 substrate peptide binding pocket (Zibetti et al., 2010). When modeled on the nucleosome, this extended loop is positioned to interact directly with the histone H2A/H2B dimer on the nucleosome in the second-site binding mode (Figure S7). This suggests a possible connection between the LSD1+8a splicing variant and the second nucleosome binding site. Unfortunately, we failed to detect H3K$_c$9me2 or H4K$_c$20me2 demethylation by LSD1+8a (experiments were performed with or without CoREST) (Figures 6A and 6C–6E). Since Laurent et al. (2015) showed that LSD1+8a requires supervilin (SVIL) and an additional factor to demethylate H3K9me2, we also performed the LSD1+8a H3K$_c$9me2 demethylase assay, with extracts kindly provided by Yang Shi's laboratory, with the same negative results (Figure 6C). LSD1+8a H4K20me2 demethylation experiments were similarly negative. These experiments were performed with or without CoREST to stabilize LSD1+8a but without additional cellular factors since LSD1+8a was reported to be sufficient to demethylate H4K20me2 on nucleosome substrates (Figure 6E). We considered the possibility that the methyl lysine analog used in our H3K$_c$9me2 and H4K$_c$20me2 adversely affected LSD1+8a demethylation activity. However, we find that LSD1+8a is unable to demethylate true H3K9me2 and H4K20me2 nucleosomes (Figures 6C and 6E). Our failure to reproduce previously published H3K9me2 and H4K20me2 demethylation by LSD1 and LSD1+8a unfortunately prevents us from determining whether the second LSD1 binding site on the nucleosome plays a role in H3K9me2 or H4K20me2 demethylation.

DISCUSSION

Many chromatin enzymes are multisubunit complexes in which the catalytic subunit is insufficient to act on a nucleosome substrate, and additional accessory subunits are required for full activity (Balasubramanian et al., 2002; Clapier et al., 2017; Morgan et al., 2016; Paul and Bartholomew, 2018; Selleck et al., 2005). Our structural studies of the LSD1/CoREST H3K4 demethylase provides the mechanistic basis for how a non-catalytic accessory subunit (CoREST) enables the catalytic subunit (LSD1) to demethylate a nucleosome substrate. We find that CoREST confers nucleosome specificity by making critical contacts with both histone and DNA components of the nucleosome and by positioning LSD1 for additional interactions with the nucleosome. LSD1 and CoREST thus form an integral unit that interacts with and acts on the nucleosome.

An unexpected feature of the LSD1/CoREST/nucleosome structure is the positioning of the LSD1 catalytic subunit on extranucleosomal DNA 100 Å away from the nucleosome core. In all structures of chromatin enzymes bound to their nucleosome substrates that we are aware of, the catalytic domain engages with the nucleosome core. It is not clear why it might be beneficial for the LSD1 catalytic domain to be located away from the

Please cite this article in press as: Kim et al., Crystal Structure of the LSD1/CoREST Histone Demethylase Bound to Its Nucleosome Substrate, Molecular Cell (2020), https://doi.org/10.1016/j.molcel.2020.04.019

Table 1. Data Collection and Refinement Statistics

Statistic	LSD1/CoREST/NCP complex[a]
Data collection	
Space group	$P2_1$
Cell dimensions	
a, b, c (Å)	103.77, 335.77, 174.633
α, β, γ (°)	90.00, 91.07, 90.00
Resolution (Å)	20.17–4.99 (5.15–4.99)[b]
R_{merge}	0.079 (1.340)
$I / \sigma I$	8.1 (0.9)
Completeness (%)	98.2 (99.9)
Redundancy	3.5 (3.6)
R_{pim}	0.050 (0.822)
$CC_{1/2}$ (%)	99.8 (35.2)
Refinement	
Resolution (Å)	4.99
No. of reflections (total/unique)	175,610/50,659
R_{work}/R_{free}	22.91%/27.74%
No. of atoms	52,996
Protein	37,122
DNA	15,662
Ligand/ion	212
Water	0
B-factors	
Protein	398.0
DNA	456.3
Ligand/ion	411.0
Water	NA
Rmsds	
Bond lengths (Å)	0.002
Bond angles (°)	0.468
Ramachandran (%)	
Favored	95.00
Allowed	4.68
Outliers	0.32

[a]A single crystal was used for structure determination.
[b]Values in parentheses are for the highest resolution shell.

nucleosome core. One possibility is to increase specificity for H3K4 by decreasing the likelihood of demethylating other H3 lysine tail residues closer to the nucleosome core. We consider this unlikely, because structural studies show that the very N terminus of histone H3 interacts with the LSD1 catalytic binding pocket, and additional residues apparently cannot be accommodated beyond the native H3 N terminus. We have substantiated this interpretation by showing that LSD1/CoREST will not demethylate nucleosomes containing H3 with two additional amino acids at the N terminus (J.Z. and S.T., unpublished data). Thus, one reason why LSD1 is specific for H3K4 demethylation is because there is no space in the LSD1 catalytic site to fit more than 3 residues N-terminal to the target lysine for H3K4. We speculate, instead, that the LSD1 catalytic domain is positioned away from the nucleosome core to probe the accessibility of extranucleosomal DNA. Since the target of LSD1, H3K4me2, is a mark for active chromatin, nucleosomes containing H3K4me2 might be expected to be uncompacted, and the extranucleosomal DNA may be expected to be accessible.

The acidic patch on the histone H2A/H2B dimer of the nucleosome is a binding hotspot for chromatin proteins and enzymes, often via an arginine anchor interaction (McGinty and Tan, 2016). Our structure of LSD1/CoREST canonical binding to the nucleosome is consistent with our previous biochemical results that LSD1/CoREST does not interact with the nucleosome acidic patch (Kim et al., 2015). The LSD1 second binding site on the nucleosome does include the histone dimer acidic patch, but there is no LSD1 arginine nearby to contact the acidic patch. Thus, canonical binding of LSD1/CoREST to the nucleosome leaves much of the nucleosome surface accessible to other factors (Figure 1B). It is also worth noting that the much of the tower domain contributed by LSD1 and CoREST remains accessible. Thus, other chromatin factors could potentially interact with the nucleosome concurrently with LSD1/CoREST binding. For example, LSD1 and CoREST form a ternary protein complex with HDAC1 called LHC (LSD1 + HDAC1 + CoREST), itself a subcomplex of the CoREST transcription repressor complex (Wu et al., 2018). It remains to be determined whether the LHC subcomplex and the CoREST complex can bind to the nucleosome and whether they demethylate nucleosome substrates with activity similar to that of LSD1/CoREST.

The LSD2 histone demethylase shares an amine oxidase catalytic domain that is similar to that of LSD1 but lacks LSD1's tower domain. Correspondingly, LSD2 does not interact with CoREST but forms a complex with the NPAC cytokine-like nuclear factor (Fang et al., 2013). Recent cryoelectron microscopy (cryo-EM) structures of LSD2/NPAC crosslinked to nucleosome core particles show limited contacts between LSD2 and nucleosomal DNA (Marabelli et al., 2019). Comparisons between the LSD1/CoREST/nucleosome and LSD2/NPAC/nucleosome structures show no discernible similarities in how the homologous LSD1 amine oxidase domains are oriented with respect to the nucleosome (Figures S4G–S4L). In particular, the LSD2 residue counterparts to the LSD1 K355, K357, and K359 residues that bind extranucleosomal DNA are oriented away from nucleosomal DNA in the LSD2/NPAC/nucleosome structure. This suggests that LSD1 and LSD2 use different mechanisms for nucleosomal interactions, despite their similar catalytic domains.

Our finding that the K661A putative, catalytically inactive mutant of LSD1 possesses significant H3K4 demethylase activity on nucleosome substrates highlights the potential pitfalls of interpreting results using histone peptide or individual histone substrates for chromatin enzymes. The LSD1 K661A mutant, found to possess essentially no H3K4 demethylase activity when assayed on histone H3 peptide or protein substrates, has been used as a catalytically inactive mutant for *in vivo* studies. Some of these studies have found that LSD1 K661A could rescue the loss of LSD1 equally as well as wild-type LSD1 could and, therefore, concluded that LSD1's demethylase activity was not required for LSD1's function in cells

(Carnesecchi et al., 2017a; Hatzi et al., 2019; Maiques-Diaz et al., 2018a, 2018b; Pilotto et al., 2015; Sehrawat et al., 2018). In light of our results, it would be prudent to re-examine the interpretation of experiments using LSD1 K661A as a catalytically inactive mutant.

In addition to the "canonical" binding of LSD1/CoREST shown in Figures 1, 2, and 3, we observed a second binding site for LSD1 to the nucleosomal histone surface in our crystals. We further establish that LSD1 binds to this second nucleosome site in solution, showing that the interaction is not simply a crystal artifact. What we have not established is the physiological relevance of this second binding mode of LSD1 with the nucleosome. Our hypothesis is that the second LSD1 binding site on the nucleosome is used for H3K9 or H4K20 demethylation. Unfortunately, we have not been able to test this hypothesis, because we have been unable to reconstitute H3K9 or H4K20 demethylation *in vitro*. It is possible that additional factors beyond what we have used are required for H3K9 or H4K20 demethylation. It is also possible that post-translational modifications of LSD1 not present in our LSD1 expressed in *E. coli* play critical roles for H3K9 or H4K20 demethylation. The question of how LSD1 might demethylate H3K9 or H4K20 is fascinating, not the least because it is very difficult to see how LSD1 could fit the other H3 or H4 tail peptides in its peptide substrate binding pocket. As discussed earlier, LSD1 engulfs the N terminus of histone H3 to position H3K4me2 for demethylation, and there is insufficient space in the peptide substrate binding pocket to accommodate more than three residues N-terminal to the target lysine residue, as is the case with H3K4. Additional experiments will be needed to investigate the molecular mechanism of LSD1's H3K9 or H4K20 demethylase activity.

Table 1

STAR★METHODS

Detailed methods are provided in the online version of this paper and include the following:

- KEY RESOURCES TABLE
- RESOURCE AVAILABILITY
  - Lead Contact
  - Materials Availability
  - Data and Code Availability
- EXPERIMENTAL MODEL AND SUBJECT DETAILS
- METHOD DETAILS
  - Preparation of protein complexes
  - Complex reconstitution and crystallization
  - Crystallographic methods
  - LSD1/CoREST Amplex Red demethylation assay
  - LSD1/CoREST western blot demethylation assay
  - HI-FI nucleosome binding assay
- QUANTIFICATION AND STATISTICAL ANALYSIS

SUPPLEMENTAL INFORMATION

Supplemental Information can be found online at https://doi.org/10.1016/j.molcel.2020.04.019.

ACKNOWLEDGMENTS

We gratefully acknowledge Michael Doyle, Gabe Epstein, Jeffrey Hall, Maxwell Kruse, Lauren McCarl, Kevin Thyne, and Bryan Tornabene for superb technical assistance; James Johnston, Turner Pecen, and Victoria Spadafora for reagent preparation; Blaine Bartholomew and Matthew Jennings for early contributions to this project; and Rob McGinty, other members of the Tan laboratory, and the Penn State Center for Eukaryotic Gene Regulation for suggestions and discussions. We also thank Benoît Laurent and Yang Shi for sharing reagents. We thank the staff of APS beamlines 24-ID-C and 24-ID-E for their help during synchrotron data collection using NE-CAT beamlines (GM124165), a Pilatus detector (RR029205), and an Eiger detector (OD021527) at the APS (DE-AC02-06CH11357). This work was supported by Estonian Research Council grant PUTJD906 to P.E. and by NIH NIGMS grants R01 GM088236, R01 GM111651, and R35 GM127034 to S.T.

AUTHOR CONTRIBUTIONS

S.-A.K. performed biochemical, crystallization, and crystallographic experiments. J.Z. performed biochemical experiments. S.-A.K., J.Z., and N.Y. solved and refined the LSD1/CoREST/191-bp nucleosome crystal structure. P.E. improved the LSD1/CoREST/189-bp nucleosome crystal molecular replacement model. S.T. conceived the experiments, provided reagents, supervised the project, wrote the manuscript, and secured funding.

DECLARATION OF INTERESTS

The authors declare no competing interests.

Received: October 31, 2019
Revised: March 2, 2020
Accepted: April 15, 2020
Published: May 11, 2020

REFERENCES

Amano, Y., Kikuchi, M., Sato, S., Yokoyama, S., Umehara, T., Umezawa, N., and Higuchi, T. (2017). Development and crystallographic evaluation of histone H3 peptide with N-terminal serine substitution as a potent inhibitor of lysine-specific demethylase 1. Bioorg. Med. Chem. *25*, 2617–2624.

Armache, K.-J., Garlick, J.D., Canzio, D., Narlikar, G.J., and Kingston, R.E. (2011). Structural basis of silencing: Sir3 BAH domain in complex with a nucleosome at 3.0 Å resolution. Science *334*, 977–982.

Balasubramanian, R., Pray-Grant, M.G., Selleck, W., Grant, P.A., and Tan, S. (2002). Role of the Ada2 and Ada3 transcriptional coactivators in histone acetylation. J. Biol. Chem. *277*, 7989–7995.

Baron, R., and Vellore, N.A. (2012). LSD1/CoREST is an allosteric nanoscale clamp regulated by H3-histone-tail molecular recognition. Proc. Natl. Acad. Sci. USA *109*, 12509–12514.

Carnesecchi, J., Cerutti, C., Vanacker, J.-M., and Forcet, C. (2017a). ERRα protein is stabilized by LSD1 in a demethylation-independent manner. PLoS ONE *12*, e0188871.

Carnesecchi, J., Forcet, C., Zhang, L., Tribollet, V., Barenton, B., Boudra, R., Cerutti, C., Billas, I.M.L., Sérandour, A.A., Carroll, J.S., et al. (2017b). ERRα induces H3K9 demethylation by LSD1 to promote cell invasion. Proc. Natl. Acad. Sci. USA *114*, 3909–3914.

Chaikuad, A., Knapp, S., and von Delft, F. (2015). Defined PEG smears as an alternative approach to enhance the search for crystallization conditions and crystal-quality improvement in reduced screens. Acta Crystallogr. D Biol. Crystallogr. *71*, 1627–1639.

Chen, Y., Yang, Y., Wang, F., Wan, K., Yamane, K., Zhang, Y., and Lei, M. (2006). Crystal structure of human histone lysine-specific demethylase 1 (LSD1). Proc. Natl. Acad. Sci. USA *103*, 13956–13961.

Clapier, C.R., Iwasa, J., Cairns, B.R., and Peterson, C.L. (2017). Mechanisms of action and regulation of ATP-dependent chromatin-remodelling complexes. Nat. Rev. Mol. Cell Biol. *18*, 407–422.

D'Arcy, A., Sweeney, A.M., and Haber, A. (2004). Practical aspects of using the microbatch method in screening conditions for protein crystallization. Methods *34*, 323–328.

Emsley, P., and Cowtan, K. (2004). Coot: model-building tools for molecular graphics. Acta Crystallogr. D Biol. Crystallogr. *60*, 2126–2132.

Fang, R., Chen, F., Dong, Z., Hu, D., Barbera, A.J., Clark, E.A., Fang, J., Yang, Y., Mei, P., Rutenberg, M., et al. (2013). LSD2/KDM1B and its cofactor NPAC/GLYR1 endow a structural and molecular model for regulation of H3K4 demethylation. Mol. Cell *49*, 558–570.

Forneris, F., Binda, C., Vanoni, M.A., Mattevi, A., and Battaglioli, E. (2005). Histone demethylation catalysed by LSD1 is a flavin-dependent oxidative process. FEBS Lett. *579*, 2203–2207.

Forneris, F., Binda, C., Adamo, A., Battaglioli, E., and Mattevi, A. (2007). Structural basis of LSD1-CoREST selectivity in histone H3 recognition. J. Biol. Chem. *282*, 20070–20074.

Foster, C.T., Dovey, O.M., Lezina, L., Luo, J.L., Gant, T.W., Barlev, N., Bradley, A., and Cowley, S.M. (2010). Lysine-specific demethylase 1 regulates the embryonic transcriptome and CoREST stability. Mol. Cell. Biol. *30*, 4851–4863.

Gill, S.C., and von Hippel, P.H. (1989). Calculation of protein extinction coefficients from amino acid sequence data. Anal. Biochem. *182*, 319–326.

Hatzi, K., Geng, H., Doane, A.S., Meydan, C., LaRiviere, R., Cardenas, M., Duy, C., Shen, H., Vidal, M.N.C., Baslan, T., et al. (2019). Histone demethylase LSD1 is required for germinal center formation and BCL6-driven lymphomagenesis. Nat. Immunol. *20*, 86–96.

Hino, S., Kohrogi, K., and Nakao, M. (2016). Histone demethylase LSD1 controls the phenotypic plasticity of cancer cells. Cancer Sci. *107*, 1187–1192.

Kabsch, W. (2010). Integration, scaling, space-group assignment and post-refinement. Acta Crystallogr. D Biol. Crystallogr. *66*, 133–144.

Kim, S.-A., Chatterjee, N., Jennings, M.J., Bartholomew, B., and Tan, S. (2015). Extranucleosomal DNA enhances the activity of the LSD1/CoREST histone demethylase complex. Nucleic Acids Res. *43*, 4868–4880.

Laurent, B., Ruitu, L., Murn, J., Hempel, K., Ferrao, R., Xiang, Y., Liu, S., Garcia, B.A., Wu, H., Wu, F., et al. (2015). A specific LSD1/KDM1A isoform regulates neuronal differentiation through H3K9 demethylation. Mol. Cell *57*, 957–970.

Lee, M.G., Wynder, C., Cooch, N., and Shiekhattar, R. (2005). An essential role for CoREST in nucleosomal histone 3 lysine 4 demethylation. Nature *437*, 432–435.

Liebschner, D., Afonine, P.V., Baker, M.L., Bunkóczi, G., Chen, V.B., Croll, T.I., Hintze, B., Hung, L.-W., Jain, S., McCoy, A.J., et al. (2019). Macromolecular structure determination using X-rays, neutrons and electrons: recent developments in Phenix. Acta Crystallogr. D Struct. Biol. *75*, 861–877.

Luger, K., Rechsteiner, T.J., and Richmond, T.J. (1999). Preparation of nucleosome core particle from recombinant histones. Methods Enzymol. *304*, 3–19.

Magliulo, D., Bernardi, R., and Messina, S. (2018). Lysine-Specific Demethylase 1A as a Promising Target in Acute Myeloid Leukemia. Front. Oncol. *8*, 255.

Maiques-Diaz, A., and Somervaille, T.C. (2016). LSD1: biologic roles and therapeutic targeting. Epigenomics *8*, 1103–1116.

Maiques-Diaz, A., Lynch, J.T., Spencer, G.J., and Somervaille, T.C.P. (2018a). LSD1 inhibitors disrupt the GFI1 transcription repressor complex. Mol. Cell. Oncol. *5*, e1481813.

Maiques-Diaz, A., Spencer, G.J., Lynch, J.T., Ciceri, F., Williams, E.L., Amaral, F.M.R., Wiseman, D.H., Harris, W.J., Li, Y., Sahoo, S., et al. (2018b). Enhancer Activation by Pharmacologic Displacement of LSD1 from GFI1 Induces Differentiation in Acute Myeloid Leukemia. Cell Rep. *22*, 3641–3659.

Makde, R.D., England, J.R., Yennawar, H.P., and Tan, S. (2010). Structure of RCC1 chromatin factor bound to the nucleosome core particle. Nature *467*, 562–566.

Marabelli, C., Marrocco, B., Pilotto, S., Chittori, S., Picaud, S., Marchese, S., Ciossani, G., Forneris, F., Filippakopoulos, P., Schoehn, G., et al. (2019). A Tail-Based Mechanism Drives Nucleosome Demethylation by the LSD2/NPAC Multimeric Complex. Cell Rep. *27*, 387–399.e7.

McCoy, A.J., Grosse-Kunstleve, R.W., Adams, P.D., Winn, M.D., Storoni, L.C., and Read, R.J. (2007). Phaser crystallographic software. J. Appl. Cryst. *40*, 658–674.

McGinty, R.K., and Tan, S. (2016). Recognition of the nucleosome by chromatin factors and enzymes. Curr. Opin. Struct. Biol. *37*, 54–61.

McGinty, R.K., Henrici, R.C., and Tan, S. (2014). Crystal structure of the PRC1 ubiquitylation module bound to the nucleosome. Nature *514*, 591–596.

Metzger, E., Wissmann, M., Yin, N., Müller, J.M., Schneider, R., Peters, A.H.F.M., Günther, T., Buettner, R., and Schüle, R. (2005). LSD1 demethylates repressive histone marks to promote androgen-receptor-dependent transcription. Nature *437*, 436–439.

Morgan, M.T., Haj-Yahya, M., Ringel, A.E., Bandi, P., Brik, A., and Wolberger, C. (2016). Structural basis for histone H2B deubiquitination by the SAGA DUB module. Science *351*, 725–728.

Nair, S.S., Nair, B.C., Cortez, V., Chakravarty, D., Metzger, E., Schüle, R., Brann, D.W., Tekmal, R.R., and Vadlamudi, R.K. (2010). PELP1 is a reader of histone H3 methylation that facilitates oestrogen receptor-alpha target gene activation by regulating lysine demethylase 1 specificity. EMBO Rep. *11*, 438–444.

Paul, S., and Bartholomew, B. (2018). Regulation of ATP-dependent chromatin remodelers: accelerators/brakes, anchors and sensors. Biochem. Soc. Trans. *46*, 1423–1430.

Pilotto, S., Speranzini, V., Tortorici, M., Durand, D., Fish, A., Valente, S., Forneris, F., Mai, A., Sixma, T.K., Vachette, P., and Mattevi, A. (2015). Interplay among nucleosomal DNA, histone tails, and corepressor CoREST underlies LSD1-mediated H3 demethylation. Proc. Natl. Acad. Sci. USA *112*, 2752–2757.

Pilotto, S., Speranzini, V., Marabelli, C., Rusconi, F., Toffolo, E., Grillo, B., Battaglioli, E., and Mattevi, A. (2016). LSD1/KDM1A mutations associated to a newly described form of intellectual disability impair demethylase activity and binding to transcription factors. Hum. Mol. Genet. *25*, 2578–2587.

Sehrawat, A., Gao, L., Wang, Y., Bankhead, A., 3rd, McWeeney, S.K., King, C.J., Schwartzman, J., Urrutia, J., Bisson, W.H., Coleman, D.J., et al. (2018). LSD1 activates a lethal prostate cancer gene network independently of its demethylase function. Proc. Natl. Acad. Sci. USA *115*, E4179–E4188.

Selleck, W., Fortin, I., Sermwittayawong, D., Côté, J., and Tan, S. (2005). The Saccharomyces cerevisiae Piccolo NuA4 histone acetyltransferase complex requires the Enhancer of Polycomb A domain and chromodomain to acetylate nucleosomes. Mol. Cell. Biol. *25*, 5535–5542.

Shi, Y., Lan, F., Matson, C., Mulligan, P., Whetstine, J.R., Cole, P.A., Casero, R.A., and Shi, Y. (2004). Histone demethylation mediated by the nuclear amine oxidase homolog LSD1. Cell *119*, 941–953.

Shi, Y.-J., Matson, C., Lan, F., Iwase, S., Baba, T., and Shi, Y. (2005). Regulation of LSD1 histone demethylase activity by its associated factors. Mol. Cell *19*, 857–864.

Simon, M.D., Chu, F., Racki, L.R., de la Cruz, C.C., Burlingame, A.L., Panning, B., Narlikar, G.J., and Shokat, K.M. (2007). The site-specific installation of methyl-lysine analogs into recombinant histones. Cell *128*, 1003–1012.

Stavropoulos, P., Blobel, G., and Hoelz, A. (2006). Crystal structure and mechanism of human lysine-specific demethylase-1. Nat. Struct. Mol. Biol. *13*, 626–632.

Tan, S., Kern, R.C., and Selleck, W. (2005). The pST44 polycistronic expression system for producing protein complexes in Escherichia coli. Protein Expr. Purif. *40*, 385–395.

Wang, J., Telese, F., Tan, Y., Li, W., Jin, C., He, X., Basnet, H., Ma, Q., Merkurjev, D., Zhu, X., et al. (2015). LSD1n is an H4K20 demethylase regulating memory formation via transcriptional elongation control. Nat. Neurosci. *18*, 1256–1264.

Whyte, W.A., Bilodeau, S., Orlando, D.A., Hoke, H.A., Frampton, G.M., Foster, C.T., Cowley, S.M., and Young, R.A. (2012). Enhancer decommissioning by LSD1 during embryonic stem cell differentiation. Nature *482*, 221–225.

Wu, M., Hayward, D., Kalin, J.H., Song, Y., Schwabe, J.W., and Cole, P.A. (2018). Lysine-14 acetylation of histone H3 in chromatin confers resistance to the deacetylase and demethylase activities of an epigenetic silencing complex. eLife *7*, e37231.

Yang, M., Gocke, C.B., Luo, X., Borek, D., Tomchick, D.R., Machius, M., Otwinowski, Z., and Yu, H. (2006). Structural basis for CoREST-dependent demethylation of nucleosomes by the human LSD1 histone demethylase. Mol. Cell *23*, 377–387.

Yang, M., Culhane, J.C., Szewczuk, L.M., Jalili, P., Ball, H.L., Machius, M., Cole, P.A., and Yu, H. (2007). Structural basis for the inhibition of the LSD1 histone demethylase by the antidepressant trans-2-phenylcyclopropylamine. Biochemistry *46*, 8058–8065.

Zibetti, C., Adamo, A., Binda, C., Forneris, F., Toffolo, E., Verpelli, C., Ginelli, E., Mattevi, A., Sala, C., and Battaglioli, E. (2010). Alternative splicing of the histone demethylase LSD1/KDM1 contributes to the modulation of neurite morphogenesis in the mammalian nervous system. J. Neurosci. *30*, 2521–2532.

Please cite this article in press as: Kim et al., Crystal Structure of the LSD1/CoREST Histone Demethylase Bound to Its Nucleosome Substrate, Molecular Cell (2020), https://doi.org/10.1016/j.molcel.2020.04.019

STAR★METHODS

KEY RESOURCES TABLE

REAGENT or RESOURCE	SOURCE	IDENTIFIER
Antibodies		
Rabbit polyclonal anti-H3K4me2	Active Motif	Cat#39141; RRID: AB_2614985
Mouse monoclonal anti-H3K9me2	Active Motif	Cat#39683; RRID: AB_2793304
Rabbit polyclonal anti-H4K20me2	Abcam	Cat#ab9052; RRID: AB_1951942
Mouse monoclonal anti-H4	Abcam	Cat#ab17036; RRID: AB_1209245
Rabbit polyclonal anti-H3	Abcam	Cat#ab1791; RRID: AB_302613
Mouse monoclonal anti-H3	Santa Cruz	Cat#sc-517576
Bacterial and Virus Strains		
E.coli BL21(DE3)pLysS	Invitrogen	Cat#C602003
Biological Samples		
Nucleosome, Recombinant Human, H3K9me2 dNuc, Biotinylated	EpiCypher	Cat#SKU16-0324
Nucleosome, Recombinant Human, H4K20me2 dNuc, Biotinylated	EpiCypher	Cat#SKU16-0332
Chemicals, Peptides, and Recombinant Proteins		
Superdex 200 Increase 10/300 GL	GE Healthcare	Cat#28-9909-44
Source 15Q anion-exchanger	GE Healthcare	Cat#17-0947-01
Source 15S cation-exchanger	GE Healthcare	Cat#17-0944-01
Nitrocellulose blotting membrane	GE Healthcare	Cat#10600009
Talon Superflow metal affinity	Clontech	Cat#635670
Amplex Ultrared	Life Technologies	Cat#A36006
Oregon Green 488 Maleimide	Life Technologies	Cat#O6034
Horseradish peroxidase	Sigma-Aldrich	Cat#P6782
2-Chloro-N, N-dimethylethylamine hydrochloride	Sigma-Aldrich	Cat#D141208
H3, H3 mutants	In house	N/A
H4, H4 mutants	In house	N/A
H2A	In house	N/A
H2B, H2B mutants	In house	N/A
TEV Protease	In house	N/A
LSD1, LSD1+8a and variants	In house	N/A
CoREST and variants	In house	N/A
Critical Commercial Assays		
SuperSignal West Pico PLUS Chemiluminescent Substrate	Thermo Scientific	Cat#34580
Deposited Data		
LSD1/CoREST/nucleosome structure	This paper	PDB: 6VYP
Recombinant DNA		
pST44-STRaHISNhLSD1Δ1-hCoRESTΔ2	This paper	coexpresses hLSD1Δ1 = hLSD1(171-852) and hCoRESTΔ2 = hCoREST(286-440)
pST50Tr-STRaHISNhLSD1Δ1	This paper	expresses hLSD1Δ1
pST44-STRaHISNhLSD1Δ1x17-hCoRESTΔ2	This paper	coexpresses hLSD1Δ1(K355E,K357E,K359E) and hCoRESTΔ2
pST44-STRaHISNhLSD1Δ1-hCoRESTΔ2x30	This paper	coexpresses hLSD1Δ1 and hCoRESTΔ2(K309E,K312E)
pST44-STRaHISNhLSD1Δ1-hCoRESTΔ2x25	This paper	coexpresses hLSD1Δ1 and hCoRESTΔ2(K378E,R382E)
pST44-STRaHISNhLSD1Δ1-hCoRESTΔ2x31	This paper	coexpresses hLSD1Δ1 and hCoRESTΔ2(R425E,R426E,R427E)

(*Continued on next page*)

Please cite this article in press as: Kim et al., Crystal Structure of the LSD1/CoREST Histone Demethylase Bound to Its Nucleosome Substrate, Molecular Cell (2020), https://doi.org/10.1016/j.molcel.2020.04.019

Continued

REAGENT or RESOURCE	SOURCE	IDENTIFIER
pST44-STRaHISNhLSD1Δ1-hCoRESTΔ2x33	This paper	coexpresses hLSD1Δ1 and hCoRESTΔ2(K309E,K312E, K378E,R382E,R425E,R426E,R427E)
pST44-STRaHISNhLSD1Δ1x17-hCoRESTΔ2x33	This paper	coexpresses hLSD1Δ1(K355E,K357E,K359E) and hCoRESTΔ2(K309E,K312E, K378E,R382E,R425E,R426E,R427E)
pST44-STRaHISNhLSD1Δ1-hCoRESTt10	This paper	coexpresses hLSD1Δ1 = and hCoRESTΔ10 = hCoREST(316-440)
pST44-STRHISNhLSD1Δ1x28-hCoRESTΔ2	This paper	coexpresses hLSD1Δ1(R608A,N717A,D721A) and hCoRESTΔ2
pST44-STRaHISNhLSD1Δ1x31-hCoRESTΔ2	This paper	coexpresses hLSD1Δ1(S609E,S719E,G725E) and hCoRESTΔ2
pST44-STRaHISNhLSD1Δ1x32-hCoRESTΔ2	This paper	coexpresses hLSD1Δ1(K661A) and hCoRESTΔ2
pST44-STRaHISNhLSD1Δ1x34-hCoRESTΔ2	This paper	coexpresses hLSD1Δ1(A539E) and hCoRESTΔ2
pST44-STRaHISNhLSD1Δ1x36-hCoRESTΔ2	This paper	coexpresses hLSD1Δ1(A539E,K661A) and hCoRESTΔ2
pST50Tr-xH3x3	This paper	expresses *Xenopus* H3(2-136,K4C,C110A)
pST50Tr-xH3t5x3x	This paper	expresses xH3(2-20,26-136,C110A,K4C)
pST50Tr-xH3t6x3	This paper	expresses xH3(2-20,31-136,C110A,K4C)
pST50Tr-xH3t8x3	This paper	expresses xH3(2-20,33-136,C110A,K4C)
pST50Tr-xH3t7x3	This paper	expresses xH3(2-20,36-136,C110A,K4C)
pST50Tr-xH3t10x3	This paper	expresses xH3(2-20,39-136,C110A,K4C)
pST50Tr-xH3t11x3	This paper	expresses xH3(2-20,41-136,C110A,K4C)
pST50Tr-xH3x35	This paper	expresses xH3(K4C,G13A,C110A)
pST50Tr-xH3x39	This paper	expresses x(K4C,K14A,C110A)
pST50Tr-xH3x36	This paper	N expresses xH3(K4C,R17A,K18A,Q19A,C110A)
pST50Tr-xH3x37	This paper	expresses xH3(K4C,K23A,R26A,K27A,C110A)
pST50Tr-xH3x23	This paper	expresses xH3(K9C, C110A)
pST50Tr-xH3x18	This paper	expresses xH3(K27,C110A)
pST50Trc2-xH4x14	This paper	expresses xH4(K20C)
pST50Trc4-hH2Bx3	This paper	expresses hH2B(Q48C)
pST55-16xNCP601a	Makde et al., 2010	to isolate 147 bp 601 sequence
pST103-12xNCP601a197M	This paper	to isolate 197 bp 601 sequence
pST50Tr-STRaHISNhLSD1x39	This paper	expresses full-length hLSD1
pST50Tr-STRaHISNhLSD1+8ax39	This paper	expresses full-length hLSD1+8a
pST44-STRaHISNhLSD1+8ax39-hCoREST	This paper	coexpresses full-length hLSD1+8a and full-length hCoREST
pST50Tr-STRaHSTNhERRalpha	This paper	expresses hERRα
Software and Algorithms		
RAPD	N/A	https://github.com/RAPD
XDS	Kabsch, 2010	http://xds.mpimf-heidelberg.mpg.de
PHENIX	Liebschner et al., 2019	https://www.phenix-online.org
COOT	Emsley and Cowtan, 2004	https://www2.mrc-lmb.cam.ac.uk/personal/pemsley/coot/
PyMol	Schrödinger	https://pymol.org/2/
ProFit	QuantumSoft	https://www.quansoft.com

RESOURCE AVAILABILITY

Lead Contact

Further information and requests for resources and reagents should be directed to and will be fulfilled by the Lead Contact, Song Tan (sxt30@psu.edu).

Please cite this article in press as: Kim et al., Crystal Structure of the LSD1/CoREST Histone Demethylase Bound to Its Nucleosome Substrate, Molecular Cell (2020), https://doi.org/10.1016/j.molcel.2020.04.019

Materials Availability

Unique and stable reagents generated in this study are available upon request.

Data and Code Availability

The accession number for the crystallographic coordinates of the LSD1/CoREST/nucleosome complex reported in this paper is PDB: 6VYP. Original gel data have been deposited to Mendeley Data: https://doi.org/10.17632/wj4x73mbnc.1

EXPERIMENTAL MODEL AND SUBJECT DETAILS

The *E. coli* strains TG1 and HB101 were used for recombinant plasmid construction. The *E. coli* strains BL21(DE3)pLysS and CodonPlus(DE3) were used for recombinant protein expression.

METHOD DETAILS

Preparation of protein complexes

The coding regions of human LSD1(171-852) and CoREST(286-482) were amplified from HeLa cDNA and cloned into pST50Tr vectors before subcloning into the pST44 coexpression vector for polycistronic expression (Tan et al., 2005). Point mutants were generated by PCR-based site-directed mutagenesis. HIS-tagged LSD1/CoREST complexes were expressed in BL21(DE3)pLysS *Escherichia coli* cells by IPTG induction at 23°C or by autoinduction at 37°C. LSD1/CoREST protein complexes were purified from crude extracts by metal affinity chromatography (Talon resin, Clontech), digested with tobacco etch virus (TEV) protease to remove the affinity tag and further purified over SourceQ (GE Healthcare) anion-exchange chromatography resin. Dynamic light scattering measurements of the purified wild-type and variant LSD1/CoREST complexes confirmed the absence of aggregation that could adversely affect enzymatic activity.

The expression vector for the LSD1+8a splicing variant was created by inserting the codons for Asp-Thr-Val-Lys following LSD1 codon 369 by PCR-based site-directed mutagenesis. HIS-tagged full length LSD1+8a and LSD1+8a(171-856) were expressed in Rosetta(DE3)pLysS cells at 23°C in autoinduction media, and purified by metal affinity, TEV protease cleavage to remove the HIS tag, SourceQ anion-exchange chromatography and SourceS cation-exchange chromatography. The pST50Tr T7 promoter based expression vector for human estrogen related receptor α was constructed using synthetic double-stranded DNA (IDT gBlock). The HIS-tagged protein was expressed in BL21(DE3)pLysS *E. coli* cells at 18°C using IPTG induction, and purified by metal affinity chromatography, TEV protease cleavage to remove the HIS tag, SourceS and SourceQ chromatography.

Histone mutations were generated by PCR-based site-directed mutagenesis. Recombinant *Xenopus* and human core histones and nucleosome core particles were prepared as described previously (Luger et al., 1999). All nucleosomes were purified by SourceQ anion-exchange high performance liquid chromatography. The histone H3K_c4me2, H3K_c9me2 and H4K_c20me2 dimethyl-lysine analog was prepared by chemically modifying purified recombinant H3 K4C, H3 K9C and H4 K20C proteins respectively with 2-chloro-N,N-dimethylethylamine hydrochloride (Aldrich) to produce N,N-dimethylated aminoethylcysteine modified H3 (confirmed by LC-MS) (Simon et al., 2007). True H3K9me2 (#16-0324) and H4K20me2 (#16-0332) nucleosomes were purchased from Epicypher.

Complex reconstitution and crystallization

LSD1/CoREST/nucleosomes complexes were reconstituted by mixing hLSD1(171-852, R608A,N717A,D721A)/hCoREST(286-440) protein complex with *Xenopus* nucleosomes containing Widom 601 nucleosome positioning DNA at a molar ratio of 3.3:1 enzyme:-nucleosome in 10 mM Tris-Cl pH 7.5, 75 mM NaCl, 1 mM DTT. The histone H3 K4M mutant was used to enhance binding of LSD1 to the nucleosome. The LSD1/CoREST/nucleosome was purified by Superdex 200 size exclusion chromatography in the reconstitution buffer supplemented with 0.1 mM PMSF. Pooled fractions were concentrated to ~10 mg/ml in VS500 centrifuge ultrafiltration devices (Vivascience).

Purified complexes were crystallized at 4°C using the modified microbatch procedure (D'Arcy et al., 2004) with 1 μl of ~10 mg/ml LSD1/CoREST/nucleosome complex mixed with 1 μl of 25 mM HEPES pH 7.5, 75 mM ammonium citrate, 10% PEG2000-MME (Fluka) and overlaid with 70 μl of Al's oil [1:1 mixture of silicon oil (Clearco) and mineral oil (Fisher)]. The crystals were soaked in 25 mM Bis-Tris pH 6.0, 75 mM ammonium citrate, 6% PEG2000-MME before a 50% PEG smear mixture of 10% PEG400, 10% PEG350-MME, 10% PEG550-MME, 10% PEG750-MME and 10% PEG500-DME was added in 4% increments at room temperature every 5 minutes to a final concentration of 24% (Chaikuad et al., 2015).

Crystallographic methods

X-ray diffraction data were collected at Advanced Photon Source NE-CAT beamline 24-ID-E (0.9792 Å, 100K) and processed using the RAPD software package (https://github.com/RAPD) and XDS (Kabsch, 2010). The 2.57 Å crystal structure of the human LSD1/CoREST complex (PDB: 2IW5) and the 2.50 Å crystal structure of the Widom 601 nucleosome core particle (PDB: 3IZ0) were used as starting models for molecular replacement in the PHASER component of the PHENIX suite (Liebschner et al., 2019; McCoy et al., 2007). Initially, both monoclinic and orthorhombic space groups were considered, as were different combinations of molecular replacement models with or without amino acid side chains, half or full nucleosome core particles, LSD1 with or without CoREST

Please cite this article in press as: Kim et al., Crystal Structure of the LSD1/CoREST Histone Demethylase Bound to Its Nucleosome Substrate, Molecular Cell (2020), https://doi.org/10.1016/j.molcel.2020.04.019

or CoREST lacking the C-terminal SANT2 domain. The best solutions as judged by molecular replacement log-likelihood gain score and mild crystal packing clashes were refined in PHENIX and analyzed using COOT (Emsley and Cowtan, 2004). The asymmetric unit of the best solution at this stage contained two molecules of LSD1/CoREST and two nucleosome core particles in $P2_1$ space group. Removing the CoREST SANT2 helical residues 412-440 for which poor electron density was available and repeating molecular replacement produced electron density for a third LSD1/CoREST molecule. The use of B-sharpened, blurred and omit maps enabled improved fit of secondary structures into the electron density map in COOT, followed by the identification of a fourth LSD1/CoREST molecule. The removed CoREST SANT2 residues 412-440 were then manually built back into the electron density.

A combination of different approaches were used to refine the structure at the relatively low resolution of 5.0 Å. Geometrical redundancies in non-crystallographic symmetry related molecules were constrained. TLS (translation/libration/screw vibration) rigid body refinement was employed. Group B-factor refinement and secondary structure Ramachandran plot restraints were applied. These refinement procedures together with PHENIX refinement alternating with real space refinement in COOT produced unambiguous electron density for the additional 23 bp of extranucleosomal DNA on either side of the nucleosome present in the crystal. In addition, the LSD1 FAD cofactor and the H3 peptide bound in the LSD1 active site were modeled in the structure, refined to a final R-free value of 26.3%. The high average B-factor of 415 reflects the low resolution of the diffraction data and is also consistent with the high B-factors observed in crystal structures containing the nucleosome core particle, particularly for the DNA component (Armache et al., 2011; Makde et al., 2010; McGinty et al., 2014; Morgan et al., 2016).

LSD1/CoREST Amplex Red demethylation assay

LSD1/CoREST nucleosomal histone H3 demethylation activity was measured using a peroxidase-coupled assay which monitors hydrogen peroxidase production (Kim et al., 2015). Reaction mixes (90 μl) containing 20 mM HEPES, Na pH 7.5, 50 mM NaCl, 10 μM Amplex Ultra Red (Life Technologies) and 0.76 μM horseradish peroxidase (Sigma) were aliquoted into 96-well microtiter plates equilibrated at 25°C before addition of 10 μl of 500 nM LSD1/CoREST complex to initiate the demethylase reaction. Fluorescence changes (excitation at 530 nm and emission at 590 nm) were monitored using a BioTek Synergy H4 Hybrid Multi-Mode Microplate Reader. The initial velocity rates were calculated using data obtained with the first two minutes of the reaction. Figures 2B, 3B, 3C, and 4B show demethylase data after subtracting background counts from reactions without LSD1 or LSD1/CoREST present (background counts were generally less than 3% of wild-type LSD1/CoREST).

LSD1/CoREST western blot demethylation assay

Demethylation assays of 30 μl containing 400 nM nucleosome substrate and 800 nM LSD1 or LSD1/CoREST complex were incubated at 37°C for 30 minutes in 50 mM Tris-Cl pH 8.5, 50 mM KCl, 5 mM MgCl2, 0.5% BSA and 5% glycerol. Western blots were developed using anti-H3K4me2 antibody (Active Motif #39141) or anti-H3K9me2 antibody (Active Motif #39683) before reprobing with anti-H3 antibody (Santa Cruz, #sc-517576 or Abcam #ab1791 antibody). Alternatively, anti-H4K20me2 antibody (Abcam #ab9052) and anti-H4 antibody (Abcam #ab17036) were used.

HI-FI nucleosome binding assay

The binding of LSD1/CoREST to nucleosomes was measured using the HI-FI (high throughput interactions by fluorescence intensity) assay as described previously (Kim et al., 2015). Recombinant nucleosomes containing 147 or 197 bp Widom 601 DNA and site-specifically labeled with Oregon Green 488 on H3 K27C were titrated with 5 nM to 10 μM LSD1/CoREST complex in 20 mM Tris-Cl pH 7.6, 50 mM NaCl, 5 mM DTT, 5% glycerol, 0.01% NP-40, 0.01% 3-CHAPS ([(3-cholamidopropyl)dimethylammonio]-1-propanesulfonate), 100 μg/ml bovine serum albumin and 2 mM EDTA and incubated at room temperature for 15 min. Fluorescence was monitored with excitation at 488 nm and emission at 526 nm on a Typhoon 9410 scanner (GE Healthcare). Assays were performed at least three times and the data fitted using a single binding isotherm. Fluorescence was measured using ImageQuant software and analyzed with ProFit (QuantumSoft).

QUANTIFICATION AND STATISTICAL ANALYSIS

Protein quantifications were performed using a Cary UV Spectrophotometer and calculated extinction coefficients (Gill and von Hippel, 1989).

Molecular Cell, Volume *78*

Supplemental Information

Crystal Structure of the LSD1/CoREST Histone Demethylase Bound to Its Nucleosome Substrate

Sang-Ah Kim, Jiang Zhu, Neela Yennawar, Priit Eek, and Song Tan

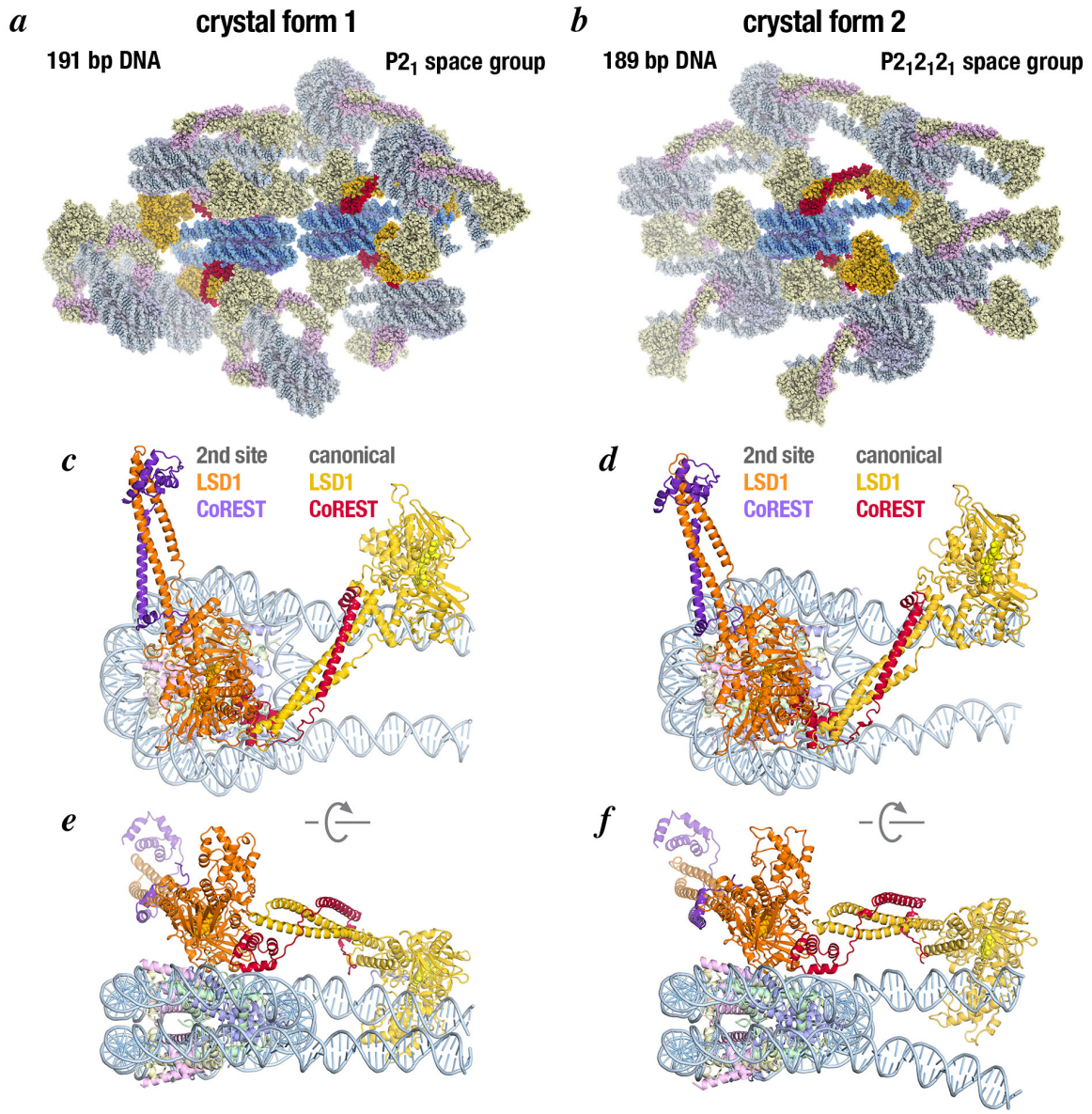

Figure S1: Distinct crystal packing but two similar nucleosome binding sites in LSD1/CoREST LSD1/CoREST/nucleosome crystal forms 1 and 2. Related to Figures 1 and 5.
(a) Crystal packing for crystal form 1 ($P2_1$ space group). LSD1, CoREST, nucleosomal histones and DNA of central asymmetric unit shown in yellow, red, purple and blue respectively, while equivalent subunits in symmetric related molecules are shown in equivalent less saturated colors. The asymmetric unit of crystal form 1 contains 2 copies of the LSD1/CoREST/nucleosome complex each with 2 molecules of LSD1/CoREST per nucleosome. (b) Crystal packing for crystal form 2 ($P2_12_12_1$ space group). Same color description as for (a). The asymmetric unit of crystal form 2 contains 2 molecules of LSD1/CoREST and 1 nucleosome. (c) The two nucleosome binding sites for LSD1/CoREST shown in Fig. 5a, b are shown on the same nucleosome for crystal form 1 (refined structure at 5 Å, contains 191 bp nucleosome DNA). The LSD1 and CoREST molecules which bind to the canonical binding site used to demethylate H3K4me2 are shown in yellow and red respectively, while the LSD1 and CoREST molecules which bind to the second site are shown in orange and purple respectively. (d) Equivalent view to (c) for crystal form 2 (partially refined molecular replacement model at 5.8 Å, 189 bp nucleosome DNA, R_{work} = 29.7%, R_{free} = 34.8%). (e) and (f) Same structures as (c) and (d), respectively, but rotated by 90°. Despite difference in crystal packing [compare (a) and (b)] and trajectory of the extranucleosomal DNA [compare (e) and (f)], LSD1/CoREST bind the nucleosome similarly both to the canonical and to the second binding site.

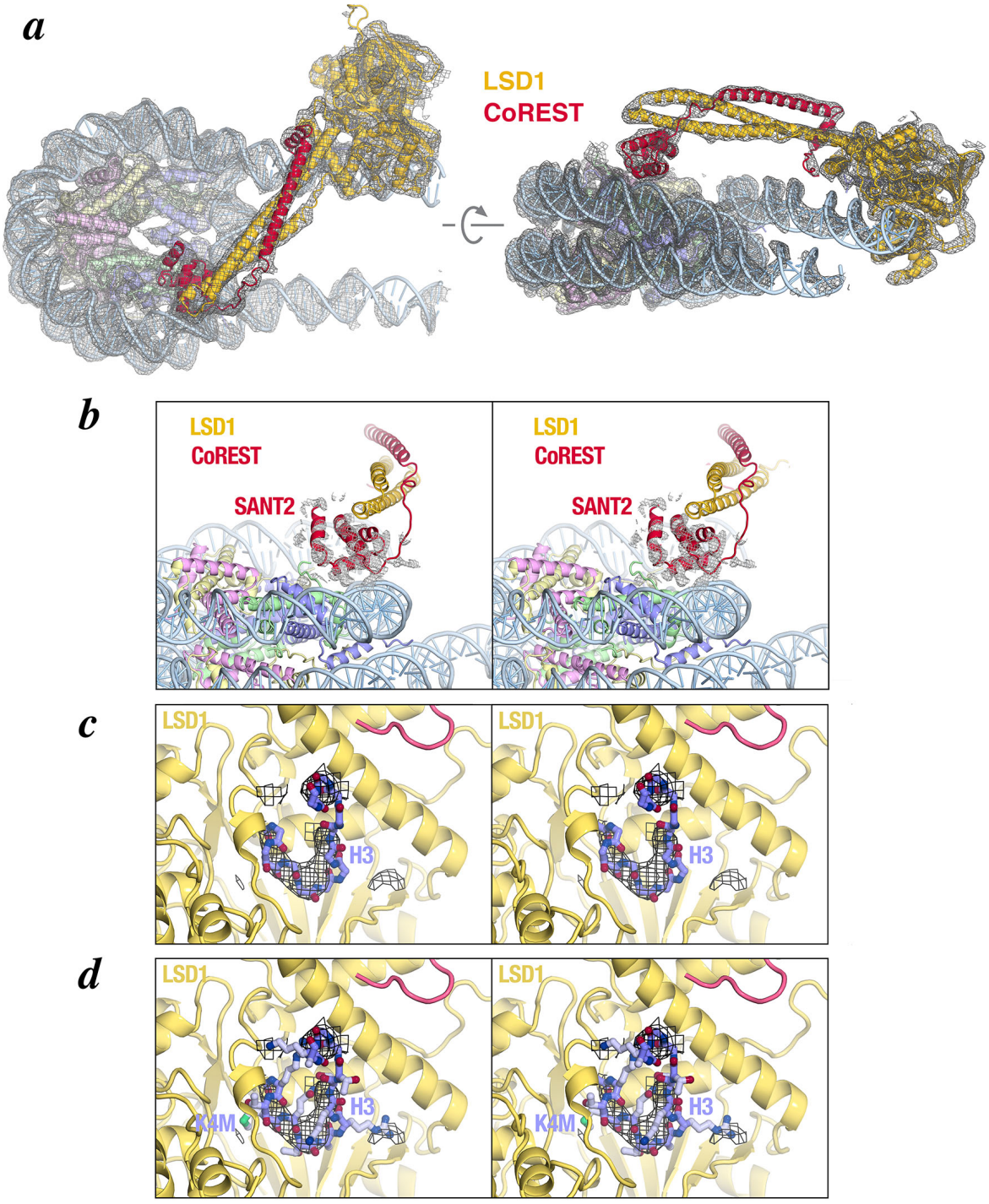

Figure S2: Electron density map for LSD1/CoREST/nucleosome complex and stereo figures for omit density maps. Related to Figure 1.
(a) $2F_o$-F_c electron density map contoured at 1 σ. Same view of structure as shown in Fig. 1b (left) and rotated by 90° (right). (b) Omit density map calculated by omitting SANT2 domain residues in all 4 copies of CoREST in LSD1/CoREST/nucleosome structure. $2F_o$-F_c map contoured at 1 σ. (c) Omit density map for H3 N-terminal tail (residues 1-15, in cornflower blue color) in LSD1 amine oxidase peptide binding pocket (in yellow) showing only the H3 main chain atoms. $2F_o$-F_c map contoured at 1 σ. (d) Equivalent omit density map to (c) except showing both H3 main chain and side chain atoms.

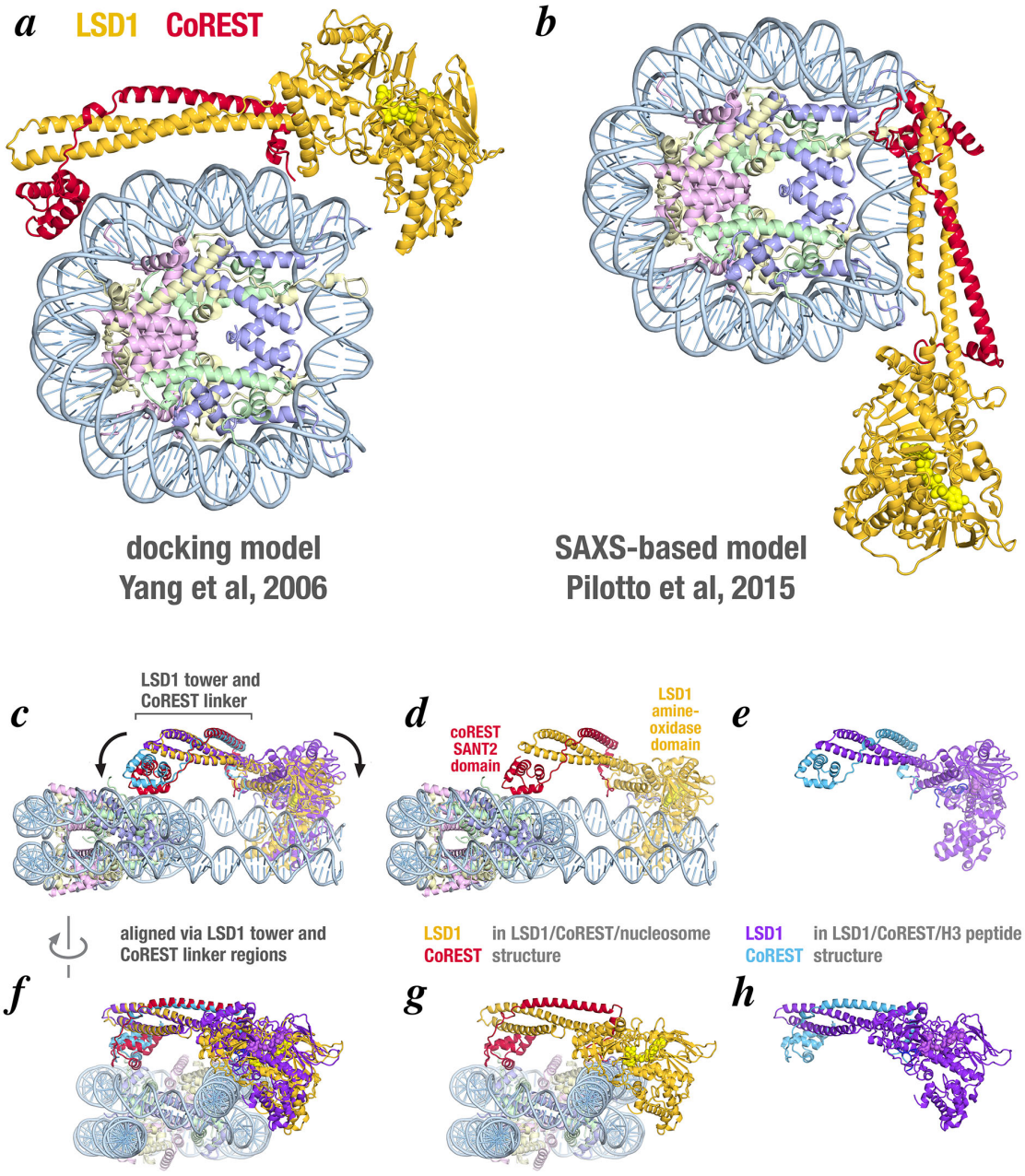

Figure S3: Previous models for LSD1/CoREST binding to the nucleosome and conformational changes in LSD1/CoREST needed to bind to the nucleosome. Related to Figure 1.
(a) Yang et al docking model based on H3 tail binding to LSD1 active site and hypothesis that CoREST SANT2 α3 helix binds to DNA major groove (figure based on Yang et al, Fig. 7). Nucleosome oriented as in Fig. 1b. (b) Pilotto et al model based on small X-ray scattering (SAXS) data (figure based on Pilotto et al, Fig. 5). (c) Superposition of LSD1/CoREST/nucleosome and LSD1/CoREST/H3 peptide structures, aligned by α-helical LSD1 tower and CoREST linker main chain atoms (rmsd = 1.1 Å). The CoREST SANT2 and LSD1 amine-oxidase domains both rotate about 5° away from the LSD1 tower/CoREST linker to bind to the nucleosome. LSD1 and CoREST in the nucleosome-bound structure are shown in yellow and red, respectively, while LSD1 and CoREST in the H3 peptide bound structure are shown in purple and sky blue respectively. (d) LSD1/CoREST/nucleosome only in same view as (c). (e) LSD1/CoREST/H3 peptide only in same view as (c). Panels (f), (g) and (h) show the respective structures except rotated 90° compared to panels (c), (d) and (e).

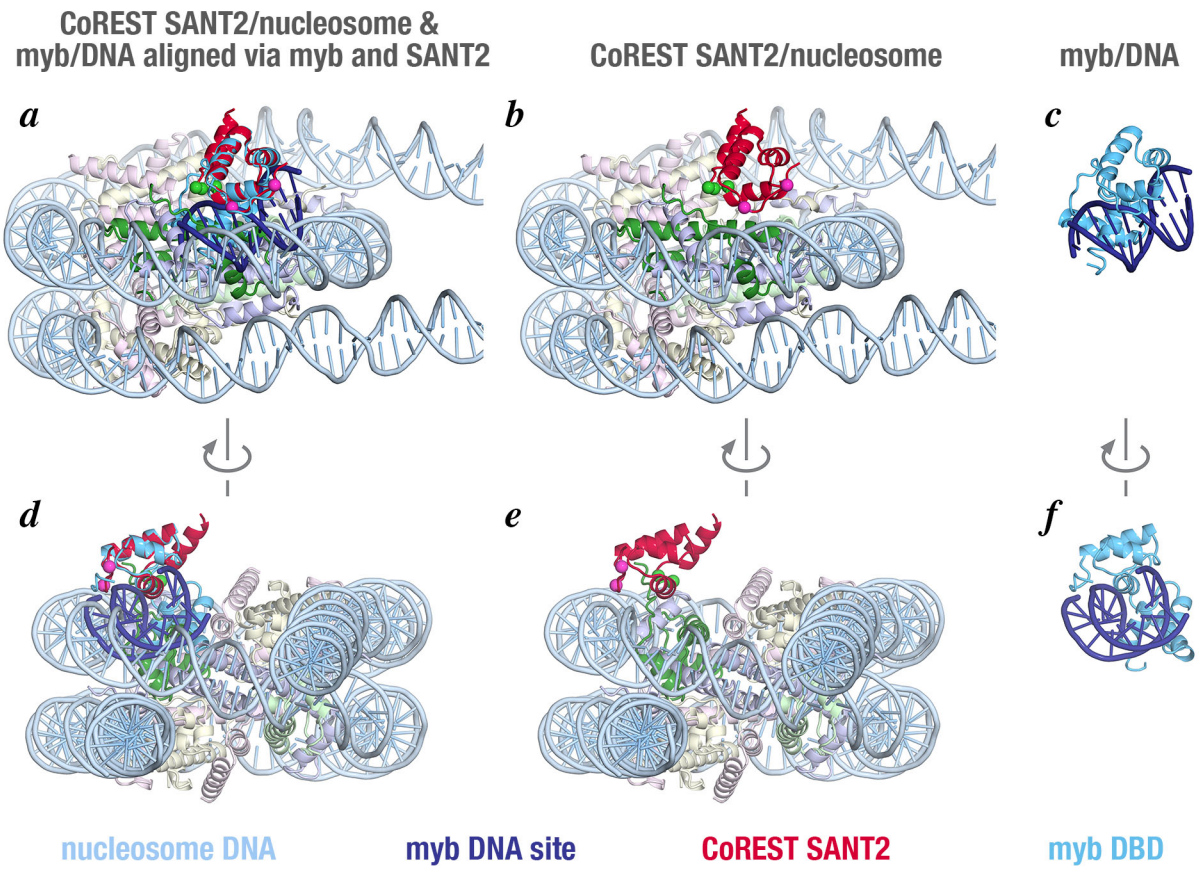
CoREST SANT2/nucleosome &
myb/DNA aligned via myb and SANT2
CoREST SANT2/nucleosome
myb/DNA
a
b
c
d
e
f
nucleosome DNA
myb DNA site
CoREST SANT2
myb DBD

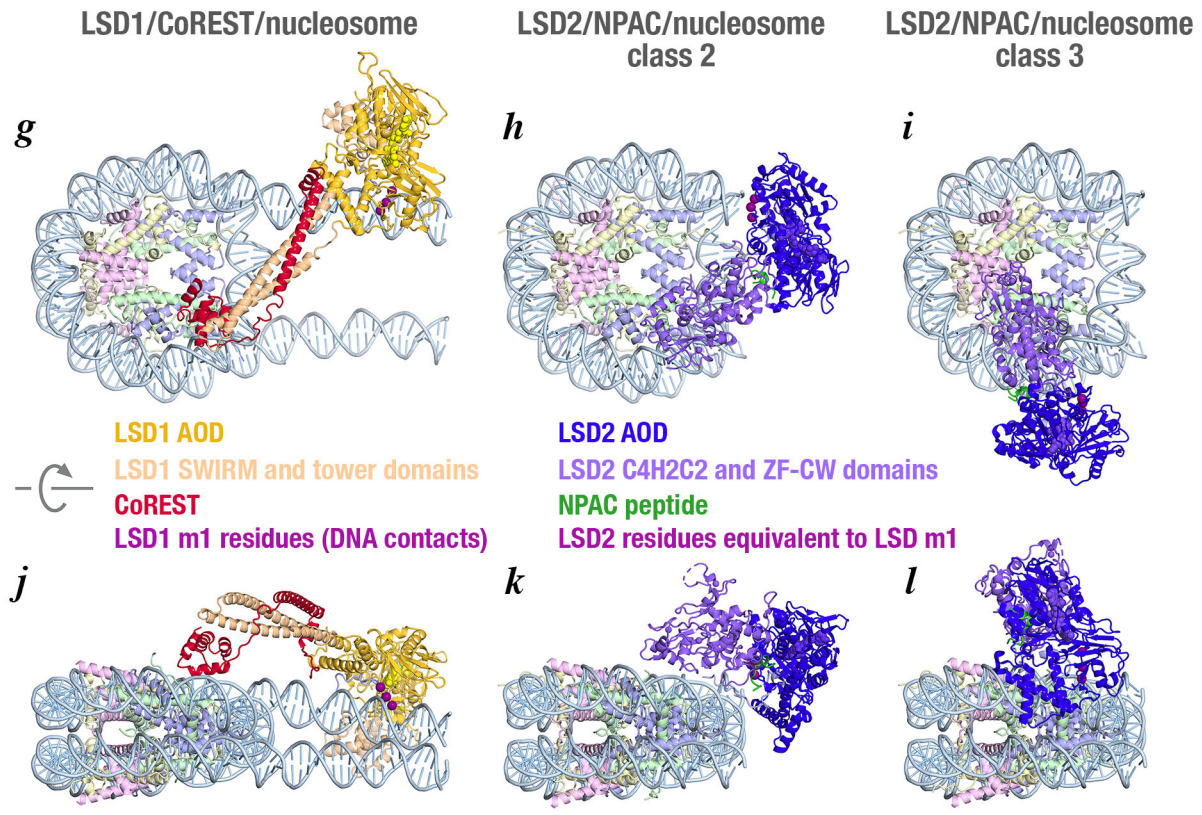
LSD1/CoREST/nucleosome
LSD2/NPAC/nucleosome
class 2
LSD2/NPAC/nucleosome
class 3
g
h
i
LSD1 AOD
LSD1 SWIRM and tower domains
CoREST
LSD1 m1 residues (DNA contacts)
LSD2 AOD
LSD2 C4H2C2 and ZF-CW domains
NPAC peptide
LSD2 residues equivalent to LSD m1
j
k
l

Figure S4: Structural comparison of CoREST SANT2 interactions with the nucleosome in LSD1/CoREST/nucleosome complex versus myb DNA-binding domain interactions with DNA in myb/DNA complex and structural comparison of LSD1/CoREST/nucleosome crystal structure and LSD2/NPAC/nucleosome cryoEM structures. Related to Figure 1.

Despite structural similarities of the CoREST SANT2 domain with the myb DNA-binding domain, the CoREST SANT2 domain does not interact with DNA like the myb DNA-binding domain does. (a) Superposition of CoREST SANT2/nucleosome from LSD1/CoREST/nucleosome structure with myb DNA-binding domain/DNA structure (PDB id 1mse), aligned via the SANT2 and myb DNA-binding domains. From the LSD1/CoREST/nucleosome structure: the CoREST SANT domain is show in red, the histone H4 subunit it contacts in green and nucleosomal DNA in light blue. The Cα atoms of CoREST m3 and m4 mutations shown in Fig. 2 are shown as pink and green spheres respectively. From the myb DNA-binding domain/DNA structure: the myb DNA-binding domain is shown in sky blue and the DNA in dark blue. (b) LSD1/CoREST/nucleosome only in same view as (a). (c) myb DNA-binding domain/DNA only in same view as (a). Panels (d), (e) and (f) show the respective structures except rotated 90° compared to panels (a), (b) and (c). (g) LSD1/CoREST/nucleosome structure in same view as Figure 1. The LSD1 amine-oxidase domain (AOD) is shown in yellow, while the LSD1 SWIRM and tower domains and the CoREST subunit are shown in peach and red respectively. The Cα atoms of the LSD1 m1 residues [Lys355, Lys357, Lys359] close to extranucleosomal DNA (Fig. 2a) are shown as purple spheres. (h) LSD2/NPAC peptide/nucleosome class 2 cryoEM structure (PDB id 6r1u) with nucleosome in same orientation as in (g). The LSD2 AOD is shown in blue, while the LSD2 C4H2C2 and ZF-CW domains and the NPAC peptide are shown in purple and green respectively. The LSD2 residues equivalent to the LSD1 m1 residues [LSD2 residues Lys460, Gly462, Arg464] are shown as purple spheres. (i) LSD1/NPAC peptide/nucleosome class 3 cryoEM structure (PDB id 6r25). Same colors are in (h). Panels (j), (k) and (l) show the respective structures in panels (g), (h) and (i) rotated by 90°.

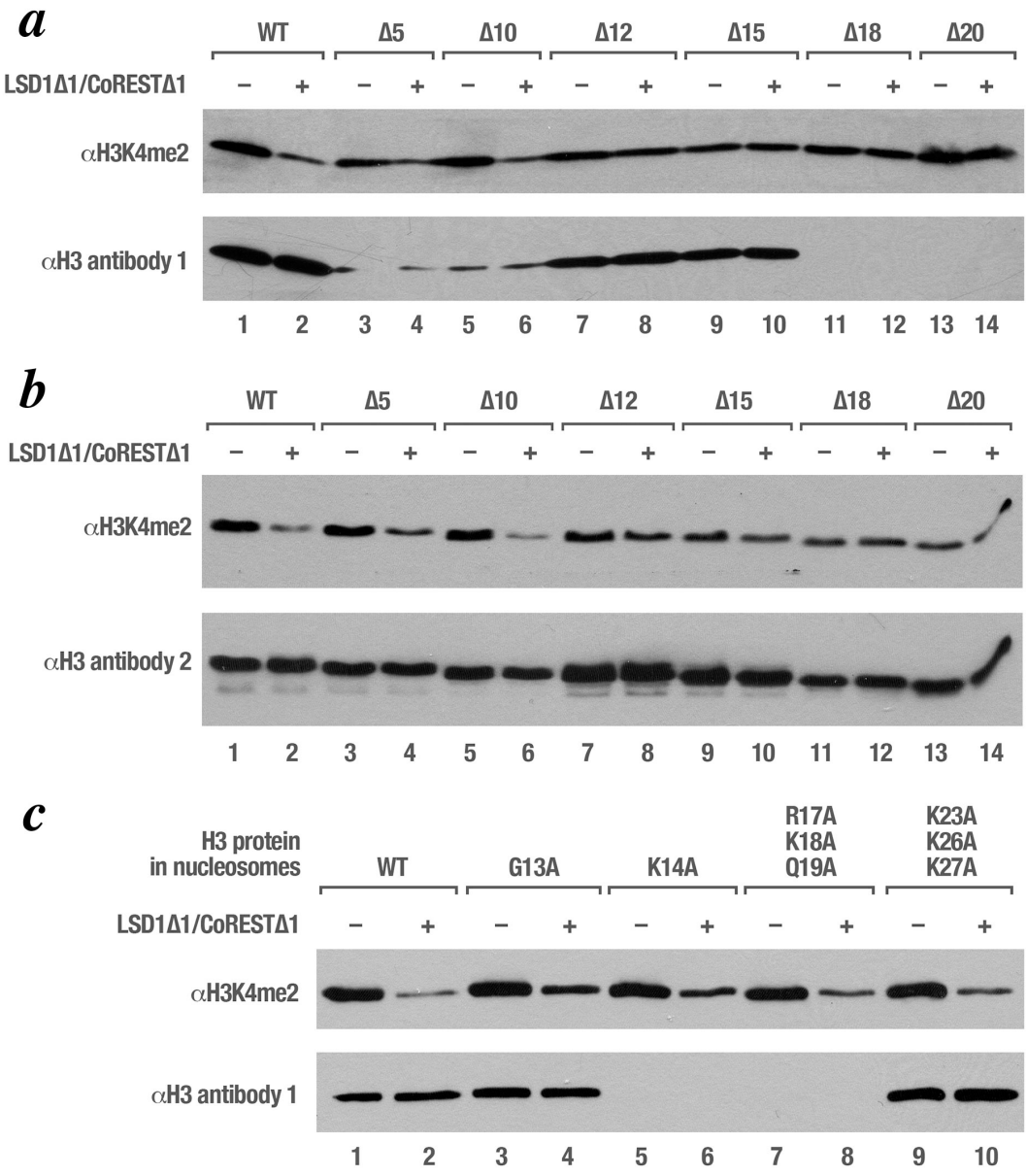

Figure S5: Histone demethylase activity of LSD1Δ1/CoRESTΔ1 on 197 bp H3K$_c$4 nucleosome substrates containing H3 tail variants analyzed by Western blotting using anti-H3K4me2 antibodies. Related to Figure 3.

(a) Histone demethylase activity on H3K$_c$4 nucleosome substrates containing 5, 10, 12, 15, 18 and 20 residue deletions starting from H3 Ala21. Some activity is detected with the Δ10 deletion, but the Δ12 deletion essentially eliminates LSD1/CoREST demethylation, consistent with our LSD1/CoREST/nucleosome crystal structure. We observe different intensity signals for the loading control reprobing using the Santa Cruz sc-517576 anti-H3 antibodies. We interpret this to indicate that the Δ5, Δ10, Δ18 and Δ20 H3 deletions remove important epitopes for this anti-H3 antibody used while the Δ12 and Δ15 H3 deletions fortuitously restore epitopes. (b) Replicate of experiment shown in (a) using the Abcam #1791 antibody. (c) Histone demethylase activity on H3K$_c$4 nucleosome substrates containing point mutations in histone H3 tail. It appears that H3 K14 and one or more of R17, K18 and Q19 constitute important residues for the Santa Cruz sc-517576 anti-H3 antibody epitope(s).

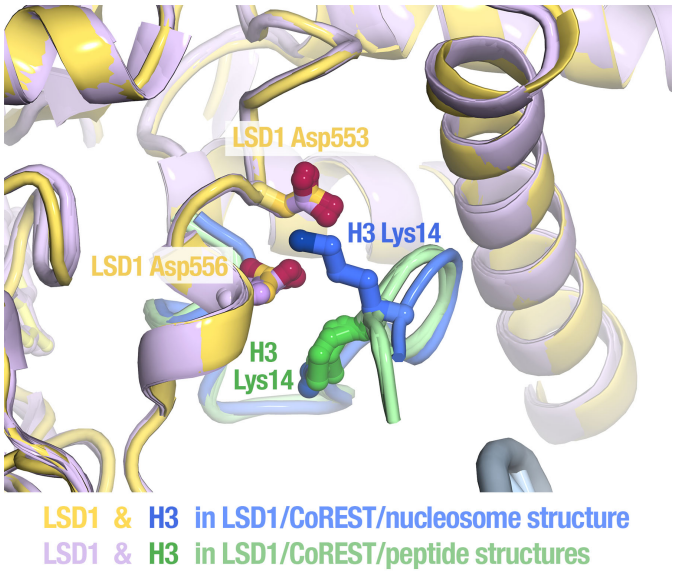

Figure S6: H3 Lys14 side chain refines in a conformation which interacts with LSD1 Asp553 and Asp556. Related to Figure 3.
Unlike other structures of LSD1/CoREST or LSD1+8a/CoREST (pink) with H3 peptides (green) (Amano et al., 2017; Forneris et al., 2007; Zibetti et al., 2010) where H3 Lys14 side chain points away from LSD1 Asp553 and Asp556 residues, H3 Lys14 side chain (blue) points to and interacts with these LSD1 residues in the LSD1/CoREST/nucleosome structure (yellow).

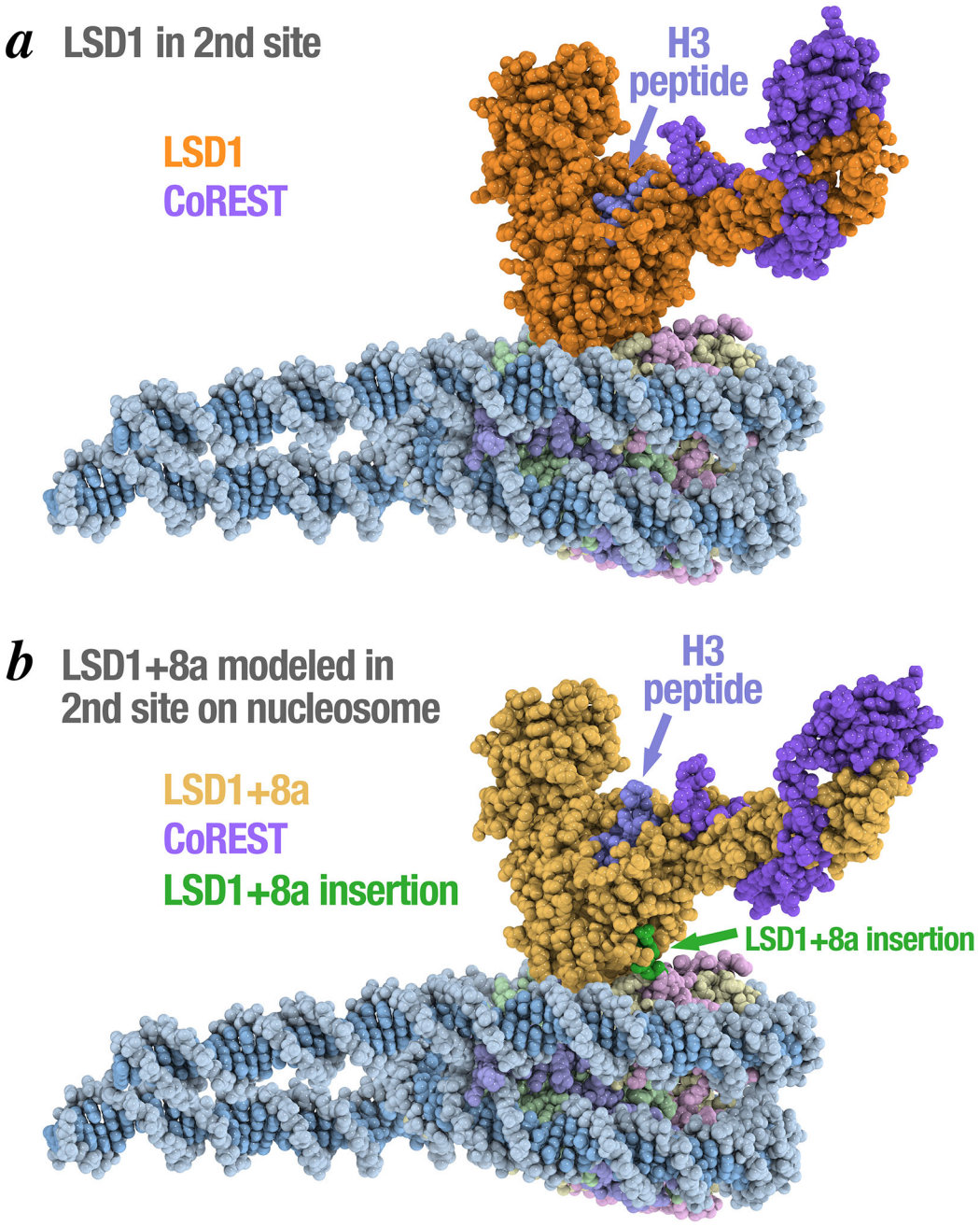

Figure S7: LSD1+8a insertion is positioned to interact with the nucleosome if LSD1+8a binds to the second LSD1 nucleosome binding site. Related to Figure 5.
(a) LSD1/CoREST/nucleosome second binding site structure with LSD1 shown in orange, CoREST in purple, H3 N-terminal peptide in light purple-blue. (b) LSD1+8a/CoREST/H3 peptide crystal structure (PDB id 2X0L) modeled in second site binding on nucleosome by aligning LSD1+8a with LSD1. LSD1+8a (shown in cornflower yellow) contains an insertion that results in a loop (in green) positioned to interact directly with histones H2A and H2B.